北京理工大學

Beijing Institute of Technology
Bachelor's Thesis

Attitude Stability Control Scheme and Simulation of Wheel-Legged Vehicles

School:	School of Mechanical Engineering
Degree:	Bachelor of Science in Mechanical Engineering
Author:	廖登廷
Student ID:	1120183302
Supervisor:	刘辉

June 5 2022

北京理工大學

Bachelor's Thesis Specifications

Category: Bachelor's Thesis

Type: Theoretic Research

Attitude Stability Control Scheme and Simulation of Wheel-Legged Vehicles

School: School of Mechanical Engineering

Degree: Bachelor of Science in Mechanical Engineering

Author: 廖登廷

Student ID: 1120183302

Supervisor: 刘辉

DESCRIPTION:

The wheel-legged platform combines the advantages of wheeled vehicles and legged robots, and has the characteristics of high mobility and high passability. , transportation, safety, special operations and social services and other fields have huge application potential. This topic mainly focuses on the characteristics of the wheel-leg platform's large-scale vehicle attitude adjustment, studies the problem of maintaining a stable and fast driving attitude under sinusoidal road conditions, and studies the kinematics and dynamic characteristics of the wheel-leg platform's secondary large-stroke actuation system. , proposed a control strategy to keep the vehicle attitude stable and fast passing, established a simulation model, and analyzed the influencing factors of the platform performance.

SPECIFICATIONS:

1. Main given conditions and basic parameters

(1) The platform has a self-weight of 50kg and a load of 10kg;

(2) The continuous torque of the joint motor is 50Nm, the peak torque is 150Nm, and the output speed is 250r/min;

(3) The continuous torque of the wheel motor is 9Nm, the peak torque is 27Nm, and the output speed is 1000r/min;

(4) The thigh length is 290mm, the calf length is 280mm, and the wheel diameter is 200mm.

2. Design analysis content and job requirements

(1) According to the application background and requirements, study the mechanism and method of vehicle attitude stabilization adjustment of wheel-leg platform, and analyze the difficulties and solutions of vehicle attitude stabilization adjustment on sinusoidal road surface (design/development solution capability);

(2) The kinematics and dynamics of the wheel-leg platform are analyzed, and the simulation model of the sinusoidal road surface and the wheel-leg platform is established. (the ability to use modern tools, research ability);

(3) Propose a vehicle attitude stability adjustment control strategy for the wheel-leg platform to pass quickly on sinusoidal roads, and study the influence of platform design

parameters on the platform's ability to pass on sinusoidal roads (research ability);

(4) Participate in the scientific research team meeting to understand the development status of the wheel-leg platform and key bottleneck technologies (communication ability);

(5) Check the literature, think about the application prospects of the wheel-leg platform, fill in the weekly records on time, and learn the relevant simulation and analysis software. (Lifelong Learning Ability)

3. Form of achievement and workload

(1) The number of words in the graduation thesis (including the software design manual) shall not be less than 25,000 words;

(2) Review more than 25 documents (monographs and textbooks are not included, and at least 8 foreign language documents);

(3) Write a literature review of no less than 7,000 words;

(4) Translate foreign language materials related to the project with a word count of not less than 5,000 words;

(5) The computational workload of experiments and research shall not be less than 8 weeks;

(6) The amount of completed drawings shall not be less than 1 drawing which is converted into a drawing of size A0.

Supervisor 刘游 Date June/06/2022

Header of Institute _____ Date _____

Program Leader _____ Date _____

原创性声明 Statement of Originality

本人郑重声明：所呈交的毕业设计（论文），是本人在指导老师的指导下独立进行研究所取得的成果。除文中已经注明引用的内容外，本文不包含任何其他个人或集体已经发表或撰写过的研究成果。对本文的研究做出重要贡献的个人和集体，均已在文中以明确方式标明。特此申明。

I, 廖登廷, solemnly declare: the submitted graduation design (thesis), is the research achievement completed independently by myself under the guidance of the supervisor. This article does not contain any research published or written by any other individual or group, except as already referenced in this paper. Individuals and groups that have made important contributions to the study of this paper are clearly indicated and cited in the paper.

Student (Signature): 廖登廷 Date: June/06/2022

关于使用授权的声明 State of Use Authorization

本人完全了解北京理工大学有关保管、使用毕业设计（论文）的规定，其中包括：①学校有权保管、并向有关部门送交本毕业设计（论文）的原件与复印件；②学校可以采用影印、缩印或其它复制手段复制并保存本毕业设计（论文）；③学校可允许本毕业设计（论文）被查阅或借阅；④学校可以学术交流为目的，复制赠送和交换本毕业设计（论文）；⑤学校可以公布本毕业设计（论文）的全部或部分内容。

I fully understand the regulations on the storage, use of graduation design (thesis) in Beijing Institute of Technology. Beijing Institute of Technology has the right to (1) keep, and to the relevant departments to send the original or copy of this graduation design (thesis); (2) copy and preserve this graduation design (thesis) by photocopying, miniature or other means of reproduction; (3) allow this graduation design (thesis) to be read or borrowed; (4) for the purpose of academic exchange, copy, give and exchange this graduation design (thesis); (5) publish all or part of the contents of this graduation design (thesis).

Student (Signature): 廖登廷 Date: June/06/2022

Supervisor (Signature): 刘源 Date: June/06/2022

Attitude Control Scheme and Simulation of Wheel-Legged Vehicles

Abstract

Wheel-legged vehicles combine the benefits of wheeled vehicle, and legged robots, which means wheel-legged vehicles are not only rapid and smooth, but also have better mobility and can adjust attitude in a large range. The thesis introduces an attitude control scheme for wheel-legged vehicles to keep the attitude stable when passing through tough terrains, which can make the vehicles more reliable in planetary exploration, disaster relief, battlefield rescue, volcanic exploration, carrying weapons, transporting goods and so on.

The leg mechanism of the vehicle is analyzed by virtual model control (VMC). Virtual mass-spring-damper systems are attached to legs, and the kinematics and dynamic performance of the system are analyzed. The joint motors are actuated by the torque generated from VMC, and the inverse kinematics is also applied to compensate the torque signal. The performance of the vehicle on rough terrains is simulated by sinewave terrains. The vehicle is modelled by Simscape to verify the effectiveness of attitude control scheme. It is simulated to pass through symmetric and unsymmetric sinewave terrains rapidly. The simulation results show that the attitude control scheme can hold the pitch angle, roll angle and stand height stable on sinewave terrains.

Key Words: Attitude Control; Wheel-legged Vehicle; Inverse Kinematics; VMC; Simscape

Table of Contents

Chapter 1 Introduction

1.1 Background and Significance

People usually have different requirements for different types of vehicles. There are some typical requirements like speed, mobility, stability, efficiency, trafficability and so on. Recent years, many researchers focus on the locomotion performance of various new types of vehicles in more hazardous environment like natural rough terrains. Unlike traditional off-road vehicles, with the development of science, those vehicles are conceived to be unmanned, highly mobile, and equipped with active transformable structures to overcome unknown hardships[1]. They are termed as unmanned ground mobile vehicles (UGMVs). UGMVs can be applied in more advanced missions, for instance, planetary exploration, disaster relief, battlefield rescue, volcanic exploration, carrying weapons, transporting goods and so on. According to the locomotion system and mechanism, UGMVs can be classified into 4 categories, wheeled, legged, tracked, and hybrid vehicles. Wheel-legged vehicle is just a kind of hybrid vehicles, which means the locomotion system is composed by both legs and wheels. Each kind of vehicles has their own inherent properties and features, thus being suitable in different circumstances.

Wheeled vehicle can be the most common one. Traditional off-road cars are usually equipped with internal combustion engine with large displacement, complicated hydraulic system, and well-tuned suspension system. Wheeled vehicles tend to have much higher maximum speed compared with other types of vehicles, and have higher drive efficiency.[2] Legged vehicle is one of the most popular field these years, since it has lots of advantages. Legged vehicle has the potential to adapt to wider variety of terrains, even discontinuous roads. Furthermore, compared with the continuous path generated by wheeled vehicle, legged vehicle only generates discrete foot-ground contact points, and therefore it is more environmental-friendly. However, some drawbacks like low carrying capability, high dependency on electronic devices and complicated control algorithms make it not a perfect solution. When it comes to tracked vehicles, although they have high carrying capacity and

high strength, they are often used in muddy places, and always cause severe damages to the ground with low speed and loudly noise.

Wheel-legged vehicle (WLV) combines the benefits of wheeled and legged vehicles[3]. It can behave like a traditional car when it is driven only by wheels, or perform like a quadruped robot if we control the motion of legs and lock the wheels. To be more advanced, we can control both legs and wheels actively, making it adaptive to all hazardous terrains with adjustable speed, posture and attitude. The awesome mobility, trafficability and stability makes it so useful in many scientific and daily activities. Posture stability is one of the most crucial indexes to ensure its reliability in military applications, helping for disabled people, infrastructure construction, and so on.

In summary, the posture stability control has high theoretical innovation value and important engineering significance. Proper control schemes should be set up to control the posture performance of wheel-legged vehicles.

1.2 Current Research Status of Novel Mobile Vehicles

1.2.1 Research Status of Novel Wheeled Vehicles

The popular research topics of wheeled vehicles concern the design of innovative steering and suspension systems[4]. As shown in Figure 1-1, a wheeled platform, termed as 'Nomad'[5], was developed by Carnegie Mellon University in 1997. It is a four-wheel-drive vehicle and each wheel can steel separately. Equipped with transformable mechanical structure, it can change foot print and required area. Also, wheeled vehicles with passive chassis systems are under concern for higher terrain adaptability, like the 'Rocky' created by jet propulsion laboratory of California Institute of Technology[6], and 'Shrimp' developed by Swiss Federal Institute of Technology Lausanne[7], which is shown in Figure 1-2. They both have passive mobility that enable them to work in more difficult road including obstacles higher than their wheel radius. Their efficiency is clearly higher than legged vehicles with easier structure and control method.

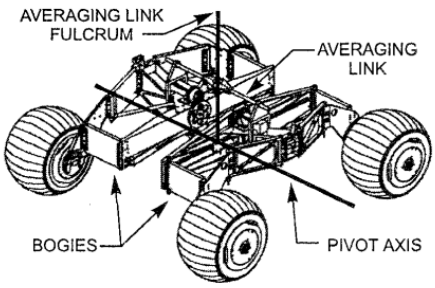

Figure 1-1 Nomad

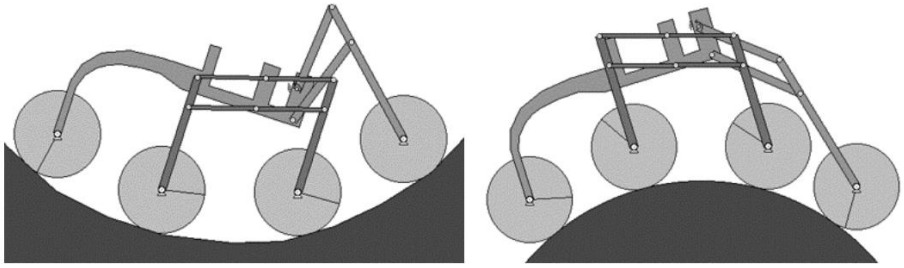

Figure 1-2 Shrimp

Domestic research on wheeled vehicle platforms started relatively late compared to foreign countries. However, with the rapid progress of technology, our country has been shrinking the technical gap from the foreign countries.

In December 2013, the first lunar rover, Jade Rabbit, in our country landed on the moon[8]. As shown in Figure 1-3, the wheeled platform weights 140 kg, and the walking mechanism is a combination of wheels and rocker arms. Each wheel can be adjusted to adapt to different heights, and can achieve 20-degree climbing and 20-cm obstacle-surmounting capabilities. The 'Jade Rabbit' lunar rover can use solar panels to absorb energy and execute actions like moving and grabbing. Its surface is made of materials that are resistant to high temperature, low temperature and radiation, so that it can work in extremely harsh environments. A robotic arm that can explore and grasp some samples.

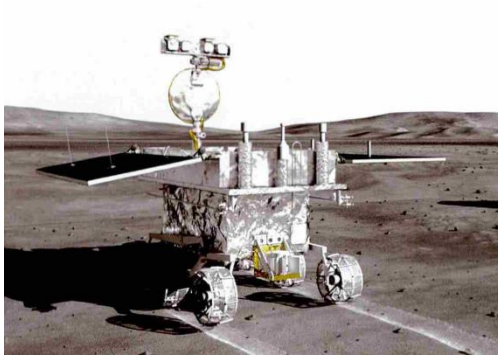

Figure 1-3 Jade Rabbit

1.2.2 Research Status of Legged Robots

Legged systems have been inspired by biological legged animals for quite a long time, and it is a rational way to increase the accessible area for mobile vehicles. Quadruped robots can be one of the most common one. In nature, animals like horses and cheetahs show great talent in running, climbing and balance themselves. They are more versatile than wheeled and tracked vehicles, and it is inherently stable compared to bipedal ones. As a result, researchers show great interests in developing quadruped robots.

'Cheetah' is one of the most famous series of quadruped robots that developed by Massachusetts Institute of Technology. The MIT Cheetah robot gives a right design approach for legged robots, it shows that electric motors can actuate incredibly fast, dynamic legged locomotion system. Taking the cheetah as the prototype for bionic research, the spine system is added to the robot, which greatly increases the stability, mobility and balance of the 'MIT Cheetah 1', shown in Figure 1-4. As the second generation of Cheetah, 'MIT Cheetah 2' can do the jump action, and it is able to jump the obstacle in front of it autonomously with maximum speed up to 6.4 m/s[9], the jump action is shown in Figure 1-5. This is benefit from the capability to mitigate high impact, and control the position and force more precisely. With 'MIT Cheetah 3', the team optimized the jump ability and jump trajectory so that the robot can jump on a 30-inch desk[10]. Besides those achievements, they are also dedicated to design a relative smaller size quadruped robot, which is called 'Mini Cheetah'. It is such a lightweight, low-cost but high-power platform, and it is the first

quadruped robot to do a 360-degree backflip from a standing position, the whole process is shown in Figure 1-7. It has similar dynamic capability as Cheetah 3, that can deliver high torque density and high tolerance to external impact[11].

Figure 1-4 MIT Cheetah 1

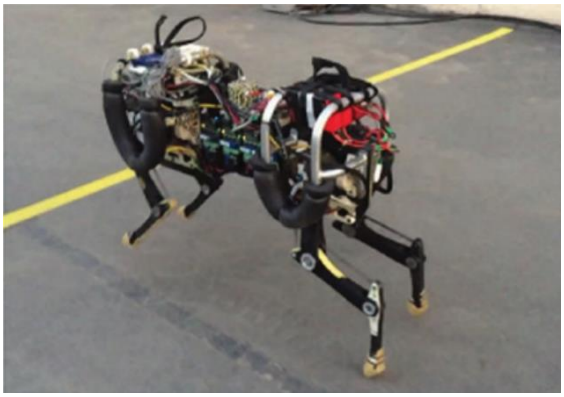

Figure 1-5 MIT Cheetah 2

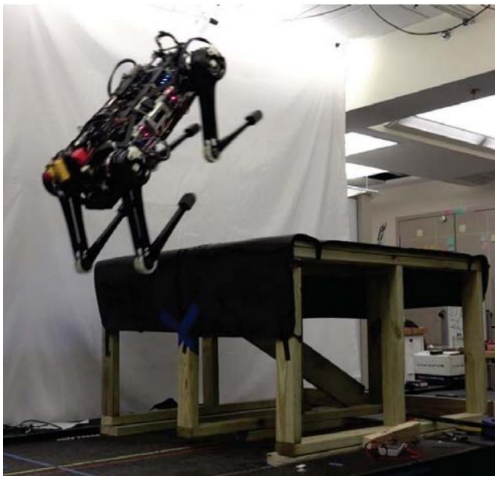

Figure 1-6 MIT Cheetah 3

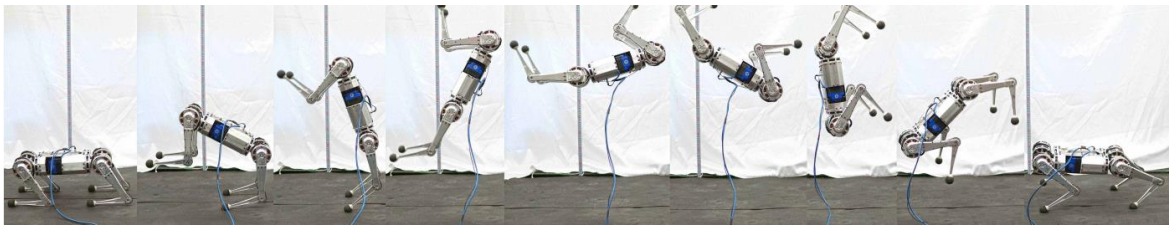

Figure 1-7 the backflip of Mini Cheetah

In September 2018, Benjamin Katz, a member of the MIT Biomimetic Robotics Lab, open-sourced the motor driver of MIT Mini Cheetah, and the code and hardware of a central board (SPIne) that connects 12 motors to the onboard computer in his graduate thesis[12]. A month later, Katz open-sourced all the code running on Mini Cheetah, which means all software and hardware of MIT Cheetah Mini are open source. That is a sensational open-source project and encourage engineers and companies all over the world to dig into the development of quadruped robots.

Boston Dynamics, a well-known robotics company in the United States, has been developing bionic robots since its establishment in 1992. 'BigDog' is one of the most well-known representative products. As shown in Figure 1-8, the single-leg system consists of one translation joint and three revolute joints, and is driven by hydraulic system with 16 degrees of freedom. Specially, a LIDAR system have been integrated onto it, which is developed by the Jet Propulsion Laboratory, to identify the environment in front of the robot and plan an ideal path, quite similar to the popular simultaneous localization and mapping technique (SLAM)[13]. 'BigDog' has the ability to cross trenches and obstacles and climb slopes quickly. It has extremely strong adaptability to the terrain environment. It can also travel on mud or snow, and can adjust its posture in time in the case of external interference. After years of experience, this company published 'Spot', shown in Figure 1-9. It is a quadruped robot launched by Boston Dynamics in 2015. It has a height of about 0.94 meters and a weight of about 75 kilograms. It can carry a payload of 45 kilograms for free movement or running. Judging from the official materials released by the company, 'Spot' climbs faster and has a more flexible gait than Big Dog. To avoid big noise, 'Spot' uses battery as a power source to drive hydraulic system, so that it can operate more quietly.

Figure 1-8 BigDog

Figure 1-9 Spot

A famous team from Zurich called ANYbotics has also been analyzing quadruped robots since 2009. The research experience is never easy, even such a large company organized by ETH Zurich has experience many trials and error. They released their first product, 'ALoF', in 2009, implementing a brand-new crawling gait that makes it dynamically stable on steep terrains[14]. The mechanical design is also impressive. They install a differential drive at the hip joint, bevel gears at the knee joint, so that 'ALoF' can show an extremely large range of reachable domain for all legs, which is shown in Figure 1-10. Subsequently, by installing springs in every joint, the durable wheel-legged platform, called 'StarlETH', is driven by series elastic actuation, shown in Figure 1-11. Next, 'ANYmal Alph' and 'ANYmal Beth', equipped with lidar based navigation, are successfully developed before their commercial product 'ANYmal B' and 'ANYmal C', the latest one is shown in Figure 1-12. The commercialized products are supposed to achieve IP67 water and dust proof, and make them truly reliable and effective in the scenes like factories by adding practical functions like auto-docking.

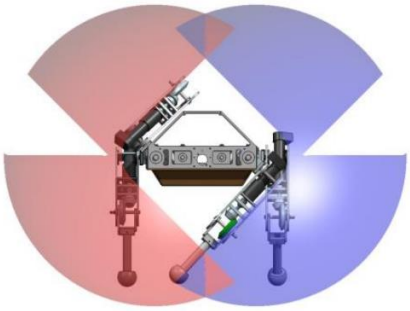

Figure 1-10 'ALoF' with a working domain

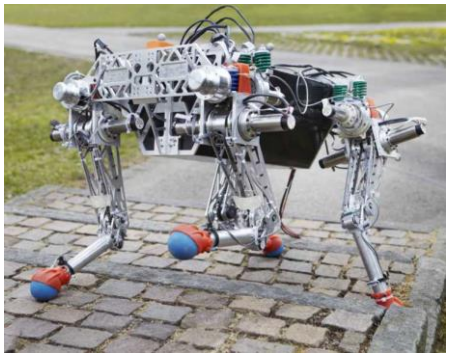

Figure 1-11 StarlETH

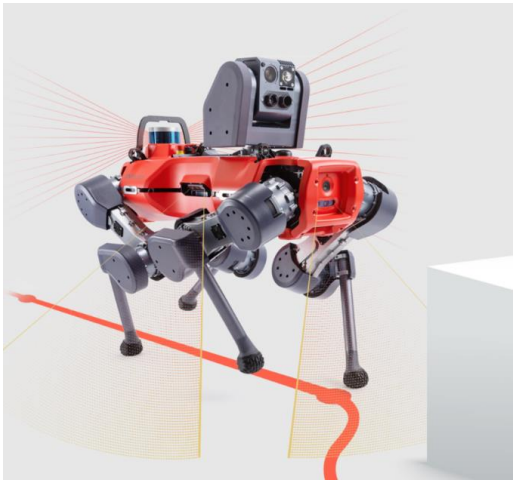

Figure 1-12 ANYmal C

China carried out the research on legged robots in the early 1990s, and many universities focus on this area. The 'Biosbot' quadruped robot developed by Tsinghua University[15], shown in Figure 1-13, 'JTUWM' robot platform developed by Shanghai Jiao

tong University[16] and 'SCalf' robot researched by Shandong University[17] are some famous domestic quadruped robots. Supported by national policies and stimulated by foreign researches, domestic researchers will go on to optimize our own robots.

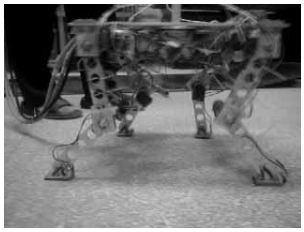

Figure 1-13 Biosbot by Tsinghua University

1.2.3 Research Status of Wheel-legged Vehicles

Wheel-legged vehicles combine the benefits of wheeled vehicle, which refers to the rapidity and smoothness, and legged robots, which refers to better mobility and less environmental damage. As a result, In the last few decades, scientists and engineers around the world have developed various kind of wheel-legged vehicles. Actually, the prototype of wheel-legged vehicles is the planetary rover that operate in the surface of other planet like Moon and Mars. The first planetary rover was launched in Nov, 1970 by the Soviet Union, called 'Lunokhod 1'. With size of 2.3 m-long, 756 kg-weight, it is driven by electric motors and use a rechargeable lunar battery as the source, which is shown in Figure 1-14. As an improved version, 'Sojourner', the first wheel-legged vehicles on Mars, with six wheels shown in Figure 1-15, has an advanced suspension that provides independent degrees of freedom for each wheel to move vertically, and it is able to come across obstacles more than 20 centimeters height[18]. Those more advanced planetary rovers are supposed to be reliable to achieve research aims, including measurement, placement of instruments. Furthermore, they must be able to locate themselves without the help of external devices like the camera on the lander. For example, a long-range rover called 'Rocky-7'[6] managed for National Aeronautics and Space Administration (NASA) , shown in Figure 1-16, achieved those goals.

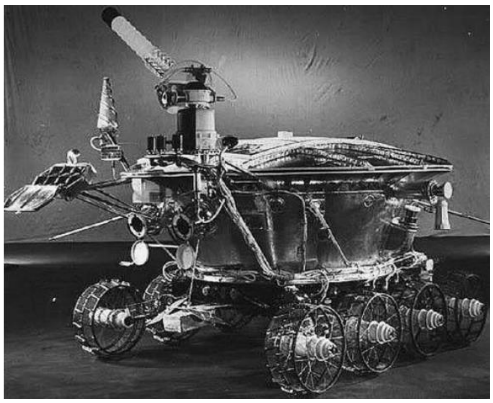

Figure 1-14 Lunokhod 1

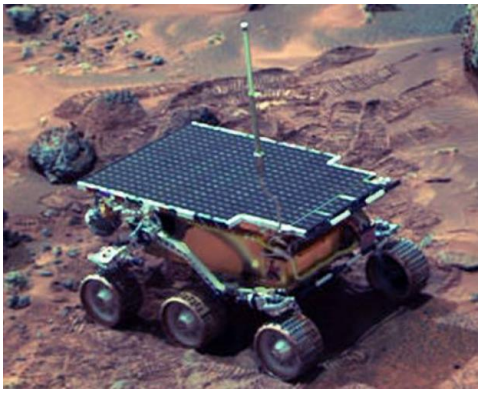

Figure 1-15 Sojourner

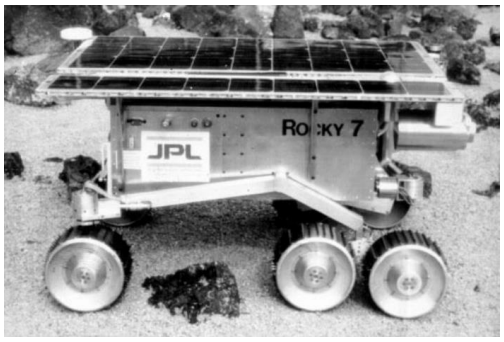

Figure 1-16 Rocky -7

'Roller Walker' is a hybrid vehicle with 4 wheels attached to the end of each leg[19]. By changing the configuration of ankle joints, the vehicle can shift the mode from walking to skating. The team from Tokyo Institute of Technology designed a novel changeover mechanism to achieve the action stated before, which is also shown in Figure 1-17. 'Hylos'

is presented by institute of Mechanics of Mosco State University with high mobility to shift to various locomotion modes according to the features of the ground. All four wheels are independently driven and steerable, but the whole body is compact and lightweight, shown in Figure 1-18. In wheeled mode, the feet just turn and wheels provide traction. In legged mode, the wheel can be locked to be passive component. Those provide a spectacular dynamic performance for 'Hylos'[20]. The 'Octal Wheel' developed by Tokyo National College of Technology has a special wheel-leg mechanism that allows it to climb complex obstacles like up-stairs and down-stairs[21]. It is also equipped with PSD obstacle detection sensors, made by Sharp, to measure the distance between the forward obstacle and tires, and the detected data is used to drive its arm at proper time.

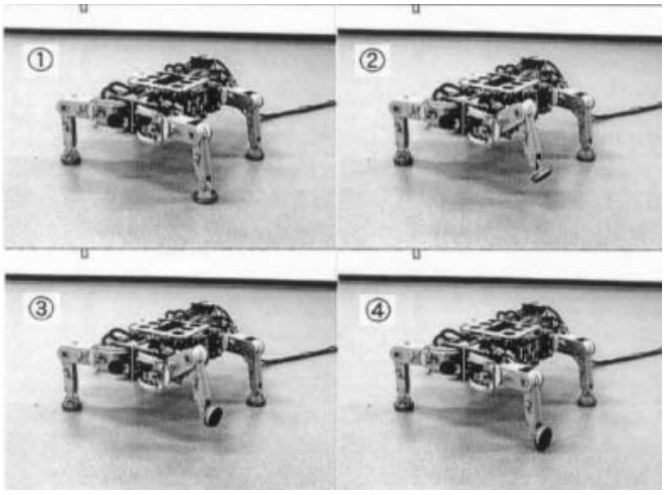

Figure 1-17 Roller Walker

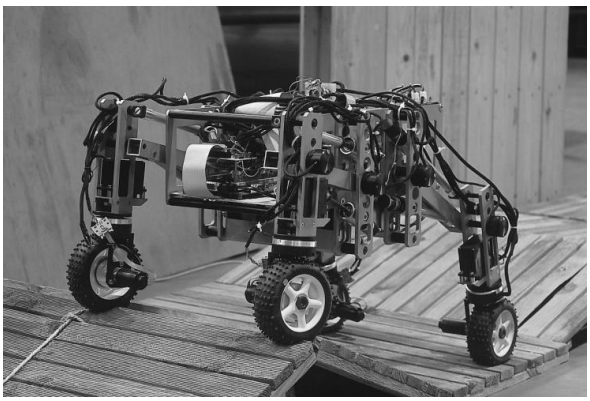

Figure 1-18 Hylos

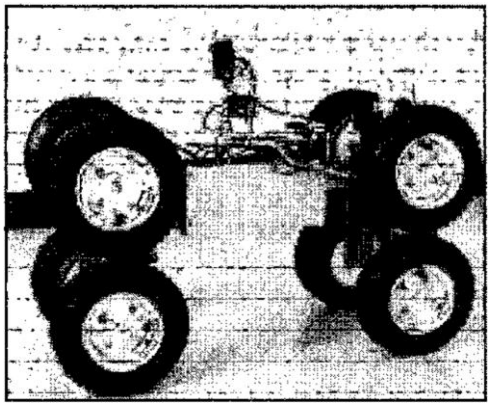

Figure 1-19 Octal Wheel

It is also worth mentioned that some advanced wheel-legged vehicles are based on the team's experience on quadruped robots. By modifying the structure of legged robots, they can inherit the properties of robot platforms. For example, ETH Zurich developed 'ANYmal on Wheels', a wheel-legged platform based on 'ANYmal' robots shown in Figure 1-20 ANYmal on wheels. Unlike some steerable wheels, their wheels are non-steerable. The vehicles travel on curves by skating, cooperate with differential steering. That must require a complex planner and controller to guide the locomotion.

Figure 1-20 ANYmal on wheels

In 2013, the University of Science and Technology of China designed the wheel-legged mobile vehicle 'HyTRo-I'. The wheels are not combined with the legs, instead, they are separated. There are 4 legs, 2 drive wheels, and 2 passive omnidirectional wheels. The wheels are arranged on symmetrical sides of the vehicle to switch motion modes, which

refers to quadruped mode, wheeled mode, and hybrid mode.

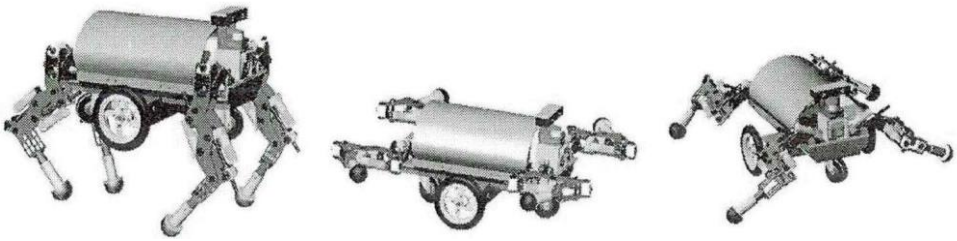

Figure 1-21 HyTRo-I

In 2017, 'BIT-NAZA' was developed by Beijing Institute of Technology. Equipped with 6-DOF parallel mechanisms as legs and 4 drive wheels, it is highly flexible and capable of carrying strong load. The team proposed an adaptive variable impendence control scheme to maintain a horizontal position of the platform thus increasing the stability[22].

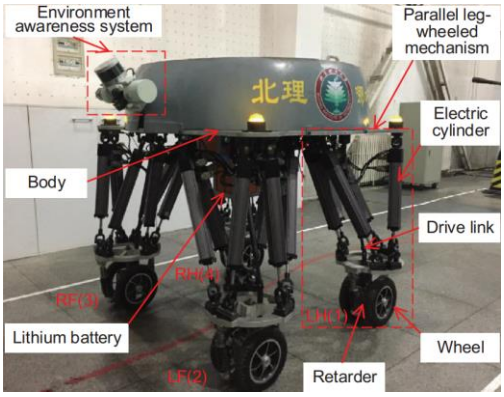

Figure 1-22 BIT-NAZA

1.3 The Overview of Current Attitude Control Research

The vehicle body of wheel-legged mobile vehicle is supported by leg systems. By controlling the lifting and dropping of leg systems, the vehicle can reach many leg-locomotion mode to control the posture of the body. Generally, there are some common features of wheel-legged vehicles listed below.

1. Each wheel can drive independently to provide traction for the vehicle.
2. Each joint angles can be independently controlled, so that the vehicle is capable of controlling its own posture.

3. The drive system is redundant.

Researchers like BenAmar F[23] claim to set a desired vector $\mathbf{p}$ to collect geometric posture parameters like shown in the Equation (1-1). And they set the time derivative of $\mathbf{p}$ to create proportional feedback. The whole control scheme is shown in Figure 1-23.

$$\mathbf{p} = (\phi, \psi, z_g, x_1, x_2, x_3, x_4)^t \tag{1-1}$$

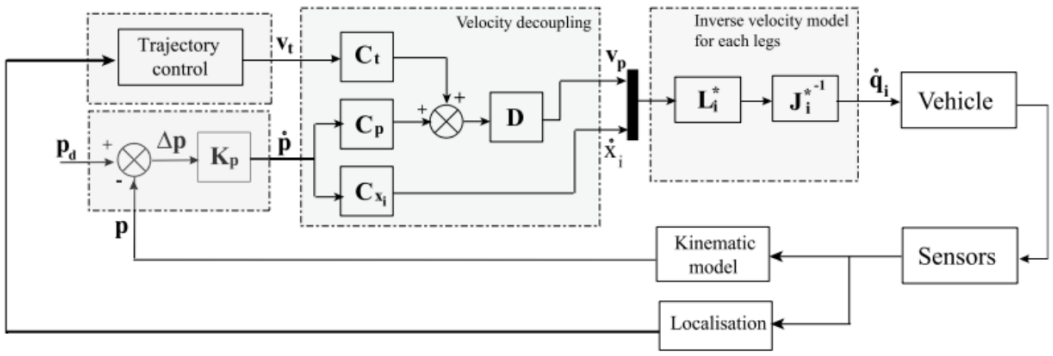

Figure 1-23 Posture control scheme with proportional feedback

The control scheme for wheeled bipedal vehicle Ascento[24], designed by the team of Klemm, differs from Hylos. Proportional feedback is replaced by LQR feedback to achieve the whole-body control (WBC). The control scheme is shown in the Figure 1-24.

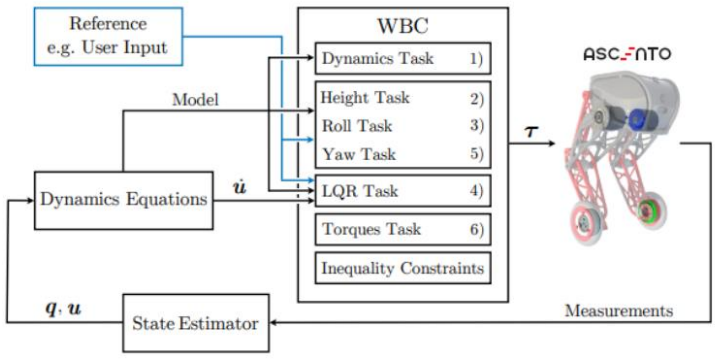

Figure 1-24 Ascento Control Method[25]

There is also a novel control method called 'intuitive control method', without any standard definition for this kind of control method. It often refers to a class of simple control

method that built up based on intuition, empirical knowledge of the system. Such methods often do not have a specific formula and there are diverse formulas, and there is even no fixed design process. Unlike enforcing the vehicle to follow a specific trajectory or enforcing the motor to reach an angle position strictly, the intuitive approach is giving instructions, or say 'suggestions', like "accelerate/decelerate for a little bit" and "raise/squat a little" to the controller according to the difference between desired state and real-time state. Actually, we human being take that kind of control method in our mind as well. When controlling our arms, instead of giving accurate torque value to each joint, the brain always gives instructions like 'higher, please', 'further, please' to dictate the position of arms, and the desired torque will be automatically computed by our muscle.[26]

The Leg Laboratory of Massachusetts Institute of Technology introduced a novel virtual control (VMC) mode for bipedal locomotion system[27]. The core of VMC is connecting linkages with imaginary virtual components like spring, damper, bearing and so on. Imaging the virtual forces generated by the virtual components exert on the object, we can control the behavior of the objective system by selecting appropriate parameters of the components like the stiffness of the virtual spring, and the damping coefficient of the damper. For more details, we can exert a vertical virtual force to support the body at a given level and exert a horizontal virtual force to pull the body to a desired velocity, and the body posture can be changed by exerting virtual torque. Researchers like Chew design a learning algorithm to change the properties of virtual components with the state of the system automatically[28]. Those control methods serve as the brain in human beings' body and Jacobian matrix works like our muscles that converts the value of forces to the value of torque. In conclusion, VMC is a simple and efficient control method that can control a mechanical system like living creatures do. Moreover, this control method can be applied to many systems without deriving exact dynamic models.

Chapter 2 Attitude Analysis

2.1 Basic Structure

According to the given specification of the wheel-legged vehicl, some essential parameters are listed in Table 2-1.

Table 2-1 Wheel-Legged Vehicle Specification

Description	Value(s)
Body mass	50 kg
Load mass	10 kg
Continuous Torque of joint motor	50 Nm
Maximum torque of joint motor	150 Nm
Rotating Speed of joint motor	250 r/min
Continuous Torque of wheel motor	9 Nm
Maximum torque of wheel motor	27 Nm
Rotating Speed of joint motor	1000 r/min
Upper leg longitudinal length	290 mm
Lower leg length	280 mm
Wheel Diameter	200 mm

There are 4 wheels in total, and each wheel is linked to the body by an upper leg (thigh) and a lower leg (calf). The joint that connects the body and upper leg is termed as hip joint, while the joint that links the upper and lower leg is called knee joint. Both are revolute joints which possess only 1 degree of freedom to rotate along their own hinge axes. Wheels are driven by wheel-side actuator, thus meaning that all joints are active, and we can control all the joints to adjust the posture of the vehicles over a much wider range than conventional vehicles. The basic structure and components of the wheel-legged vehicle are shown in Figure 2-1, labelled with corresponding numbers.

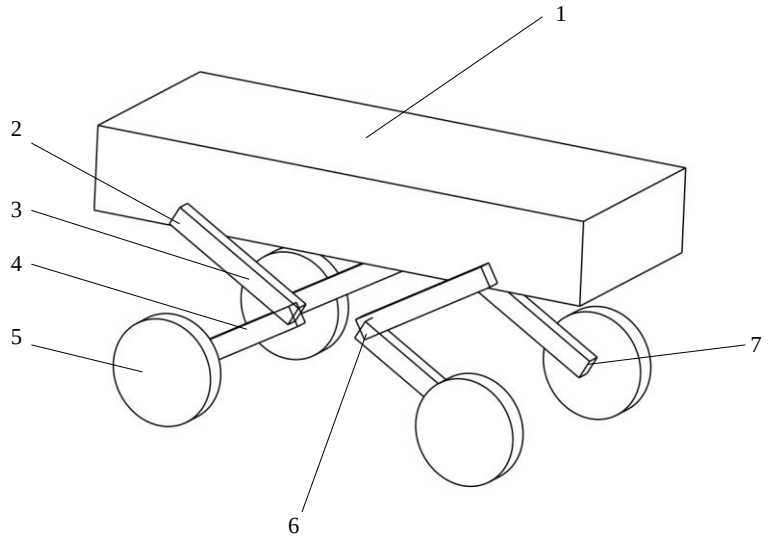

Figure 2-1 Basic components of the wheel-legged vehicle including 1-Body, 2-Hip Joint, 3-Upper Leg, 4-Lower Leg, 5-Wheel, 6-Knee Joint, 7-Wheel-side actuator

Generally speaking, there are four common configurations of the leg, which are all-elbow type, all-knee type, front-knee-rear-elbow type and front-elbow-rear-knee type. Those configurations correspond to (a), (b), (c) and (d) in Figure 2-2. The last configuration, front-elbow-rear-knee type, is chosen for this project, because that is a symmetric structure that can restrain the vibration of center of mass (COM) in the longitudinal direction caused by mechanical error and control error. Moreover, this layout makes the whole structure more compact than front-knee-rear-elbow type, with larger approach angle and departure angle, which are important evaluation parameters affecting the pass ability of this mobile vehicle.

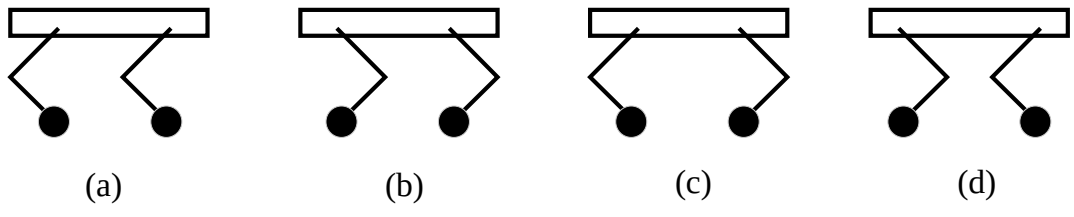

Figure 2-2 Four different layouts of legs, (a) all-elbow, (b) all-knee, (c) front-knee-rear-elbow, (d) front-elbow-rear-knee (the right side of the figure is the front side)

2.2 Set Basic Frames

In order to describe the motion of the vehicle, reasonable frames should be defined to help with the analysis. First, a fixed world frame, denoted by G_0, is essential to quantify the positions and orientations of all other frames. Next, let's define $G(x, y, z)$ as the body frame attached to the center of mass (COM) of the main body, with the positive direction of x pointing to longitudinal front side and the positive direction of z being vertically upward. As usual, y axis can be generated by setting a right-hand coordinate, which is not that important and can even be neglected in orthogonal view. The layouts of basic frames are shown in Figure 2-3.

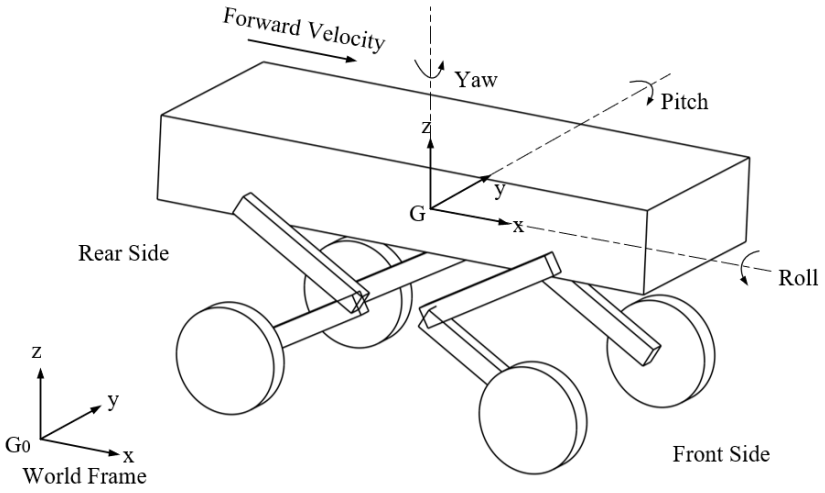

Figure 2-3 Basic frames and posture definition

2.3 Attitude Definition

The main topic of the project is the attitude of the wheel-legged vehicle, so prescribing an accurate representation method of posture at the beginning makes sense. Usually, we can use only three independent parameters to describe an arbitrary rotation accurately. There are three common representation methods, with different definition on the parameters, which refers to 'Euler Angle' method, 'Roll-Pitch-Yaw' method, and 'Axis/Angle' method.

The main feature of 'Euler Angle' method is that the followed frame always rotates about current axis, with the sequence of Z-Y-Z. Since we do not always curious about the

rotation about a principal axis, sometimes, we need to represent the rotation about an arbitrary line in space, which could be a specific edge of a cube, for instance. Different from both methods stated before, 'Roll-Pitch-Yaw' method always focus on three fixed axes that orthogonal to each other[29], which is a commonly used method to describe the posture and motion of conventional cars. Since the demand in researching the wheel-legged vehicle is not that diverse like the various types of robotic arm, 'Roll-Pitch-Yaw' method is a suitable representation method for this vehicle to evaluate the performance of it. By checking the fixed rotation axes in Figure 2-3 drawing as center lines, we can easily define the posture angles, and be careful about the positive direction of those angles are stipulated by right hand rule.

2.4 Represent Homogenous Transformation

A homogenous transformation is the combination of two kinds of basic motions, translation and rotation. In this project, the most frequently used method is how to represent the position and orientation of Frame 1 in Frame 0. Frame 0 is often regarded as a fixed frame, or base frame.

For rotation, we often use rotation matrix R_1^0 to represent the orientation of a specific coordinates 'Frame 1' with respect to 'Frame 0', and the expression of R_1^0 is shown in Equation (2-1).

$$R_1^0 = \begin{bmatrix} x_1 \cdot x_0 & y_1 \cdot x_0 & z_1 \cdot x_0 \\ x_1 \cdot y_0 & y_1 \cdot y_0 & z_1 \cdot y_0 \\ x_1 \cdot z_0 & y_1 \cdot z_0 & z_1 \cdot z_0 \end{bmatrix} \tag{2-1}$$

The elements in this matrix are all unit vectors in Frame 0 and Frame 1, so each column of rotation matrix can be regard as the projection of base vectors of Frame 1 in the direction of base vectors of Frame 0. Since dot product of any two unit vectors is the cosine value of the angle between those two vectors, the elements in rotation matrix are also termed as 'directional cosine'. Take some basic rotation motion as examples, we would some convenient result. $R_{x,\theta}$, $R_{y,\theta}$, $R_{z,\theta}$ represent the Frame 1 is generated by rotate Frame 0

along its own x, y or z axis by θ degrees.

The translation motion is relatively simpler to be represented. The translation between fixed frame 0 and follower frame 1, can be described by a simple space vector, denoted as Equation

$$R_1^0 = \begin{bmatrix} x \\ y \\ z \end{bmatrix} \tag{2-2}$$

The x, y or z value in the translation vector is the position of the origin of Frame 1 represented in Frame 0.

By combining the rotation and translation motion, people can represent a general homogeneous motion that contains both motions above more easily by integrating translation and rotation into one compound matrix, which is usually called homogeneous transformation matrix, H_1^0.

$$H_1^0 = \begin{bmatrix} R_1^0 & d_1^0 \\ o & 1 \end{bmatrix} \tag{2-3}$$

2.5 Calculating Leg Vectors according to Desired Attitude

In this section, I would introduce a method to control pitch and yaw angles by setting 'leg vector' of each leg, which is formed by the position of hip joint and wheel. Figure 2-4 shows the geometric relationships vividly. To display the geometric relationships more conveniently, I only take the front-left side as an example, neglecting the other three legs. Unlike most quadruped robot with 3 degrees of freedom for each leg, we only equip 2 actuators for each leg, thus yaw angle can only be controlled by differential steering, which is not covered in this thesis.

An intuitive idea is that the posture, including stand height, roll angle and pitch angle, can be determined by the configuration of each leg. Since the radius of these four wheels are the same, we can set a construction plane, $B_1B_2B_3B_4$, which is parallel to the ground, to simplify the following calculation process. The construction can be treated as a virtual ground, with 4 imaginary wheel-contact points denoted by B_1, B_2, B_3, B_4. A compensate

stand-height value, which equals to the wheel radius, should be added during the calculation processes.

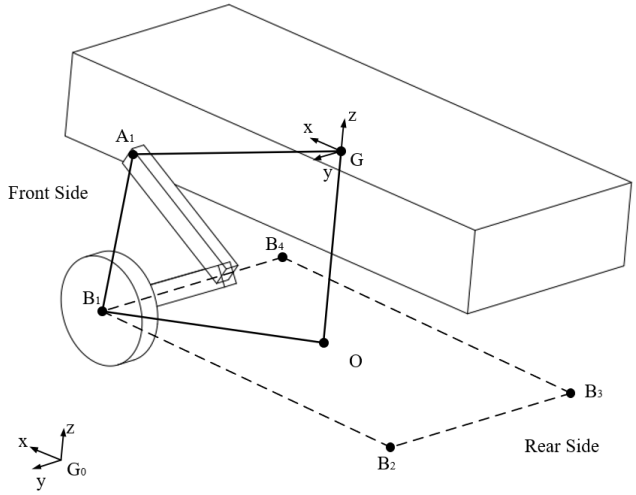

Figure 2-4 Posture Vectors

In world frame G_0, a quadrilateral in space, OGA_1B_1 is under consideration. According to simple vector addition theorem, we can get Equation (2-4).

$$\overrightarrow{GA_1} + \overrightarrow{A_1B_1} = \overrightarrow{GO} + \overrightarrow{OB_1} \tag{2-4}$$

In this formula, point O is the vertical projection of the origin point of body frame G, B_1 is the rotating center of the wheel, A_1 is the center of hip joint. Certainly, the positions of wheels are variable and can be controlled, but here, the positions of four wheels are set as known values since we must set initial positions of wheels to start the analysis. That is to say, the vector $\vec{OB_1}$ is a known vector. Similarly, the modulo of $\vec{GO}$ is the ground clearance, a value that determine the stand height of the wheel-legged vehicle, and it can also be treated as a known vector. $\vec{A_1B_1}$ is the leg vector that we desired, and it is also the vector that influence the posture of the body directly. To get $\vec{A_1B_1}$, we have to get $\vec{GA_1}$ vector according to the desired pitch angle and roll angle. Since the formulas below involves many transformation relationships between world frame and body frame, I use subscripts,

'World' and 'Body', to distinguish. Notice that $\vec{GA_1}$ is a changing vector in world frame, but it is a structural vector in body frame, which means it is constant in body frame. According to the properties of rotation matrix, we can link those two representations of $\vec{GA_1}$, the vector that connect COM with hip joint center.

$$\left(\overrightarrow{GA_1}\right)_{\text{World}} = \mathrm{R}_{\text{Body}}^{\text{World}} \left(\overrightarrow{GA_1}\right)_{\text{Body}} \tag{2-5}$$

In Equation (2-5), $\mathrm{R}_{\text{Body}}^{\text{World}}$ is the rotation matrix that transfer the representation of a specific vector from body frame to world frame, and it is directly determined by roll, pitch and yaw angles of the body.

$$\begin{aligned} R_{\text{Body}}^{\text{World}} &= R_{z,\phi} R_{y,\theta} R_{x,\psi} \\ &= \begin{bmatrix} c_\phi & -s_\phi & 0 \\ s_\phi & c_\phi & 0 \\ 0 & 0 & 1 \end{bmatrix} \begin{bmatrix} c_\theta & 0 & s_\theta \\ 0 & 1 & 0 \\ -s_\theta & 0 & c_\theta \end{bmatrix} \begin{bmatrix} 1 & 0 & 0 \\ 0 & c_\psi & -s_\psi \\ 0 & s_\psi & c_\psi \end{bmatrix} \\ &= \begin{bmatrix} c_\phi c_\theta & -s_\phi c_\psi + c_\phi s_\theta s_\psi & s_\phi s_\psi + c_\phi s_\theta c_\psi \\ s_\phi c_\theta & c_\phi c_\psi + s_\phi s_\theta s_\psi & -c_\phi s_\psi + s_\phi s_\theta c_\psi \\ -s_\theta & c_\theta s_\psi & c_\theta c_\psi \end{bmatrix} \end{aligned} \tag{2-6}$$

In Equation (2-6), $R_{z,\phi}$ indicates rotating about z axis for ϕ degree, which is yaw angle, and similarly the pitch and roll angle are denoted by θ and ψ respectively. Noted that, shorthand notation $c_\theta = \cos\theta$, $s_\theta = \sin\theta$ for the trigonometric functions in complex formulas. Then, Equation (2-4) in world frame can be rewritten as Equation (2-7).

$$(\overrightarrow{A_1B_1})_{World} = (-\overrightarrow{OG} - R_{Body}^{World} (\overrightarrow{GA_1})_{\text{Body}} + \overrightarrow{OB_1})_{World} \tag{2-7}$$

Since the vector $\overrightarrow{A_1B_1}$ in world frame is not useful in the following analysis, we are always looking for $\overrightarrow{A_1B_1}$ in hip frame, thus substituting $(\overrightarrow{A_1B_1})_{World}$ into $(\overrightarrow{A_1B_1})_{Hip}$, we can get the expressions of the desired vector shown in Equation (2-8).

$$
\begin{aligned}
(\overrightarrow{A_1B_1})_{Hip} &= R_{World}^{Hip}(\overrightarrow{A_1B_1})_{World} \\
&= R_{Body}^{Hip}R_{World}^{Body}(\overrightarrow{A_1B_1})_{World} \\
&= R_{Body}^{Hip}R_{World}^{Body}(-\overrightarrow{OG} - R_{Body}^{World}(\overrightarrow{GA_1})_{\text{Body}} + \overrightarrow{OB_1})
\end{aligned}
\tag{2-8}
$$

According to the properties of rotation matrix, R_{Body}^{World} is the inverse matrix of R_{World}^{Body}.

It is worth mentioned, that the desired attitude is measured relative to the current ground, since we assume wheels are always contacted with the current road.

In conclusion, the 'leg vector' of front-left side (FL) in the hip frame can be obtained by Equation (2-8), and the 'leg vectors' of front-right side (FR), rear-left side (RL), and rear-right side (RR) could be obtained using the same method if we input given desired roll angle, pitch angle and stand height. In brief, if we treat the method as a function, the input variables are the posture parameter, and the output value are the leg vectors of each side in their own hip frame. The method stated before is the foundation of the following researching.

Chapter 3 Inverse Kinematics

In previous chapters, I have figured out the coordinates set up of the wheel-legged vehicle, and introduced a method to look for leg vectors. Since the leg is formed by an upper leg and a lower leg, we should control the magnitude of the hip joint angle and knee joint angle. Unlike the workflow of forward kinematics, which refers to locating the wheels by joint angles, inverse kinematics is responsible to get appropriate joint angles according to the given desired locations of wheels. In brief, the 'leg vector' provided in previous chapter will be treated as input data, and this chapter will show how to control the joint angles to take wheels to their desired positions. Setting correct coordinates for legs, described in the following section, is the essential preparation for inverse kinematics analysis.

3.1 Set Denavit-Hartenberg Coordinates for Legs

Since a general homogeneous transform contains both translation and rotation, it needs 6 parameters to be fully represented. 3 parameters are used to describe rotation, like 'yaw-pitch-roll', and the other 3 parameters is responsible for translation, like 'x-y-z'. Denavit-Hartenberg convention, D-H in short, is of vital significance in engineering applications, because it can reduce the required number of parameters from 6 to 4 by selecting appropriate coordinate systems.

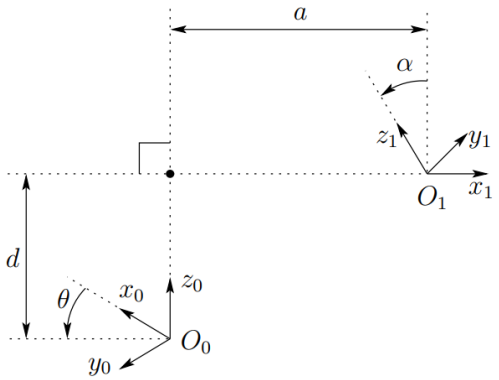

Figure 3-1 D-H convention from textbook[29]

Figure 3-1 shows how Denavit and Hartenberg stipulated the lay out of frames. To satisfy D-H convention, there are 2 requirements to be met[29].

1) The axis x_1 must be perpendicular to the axis z_0.

2) The axis x_1 must intersect with the axis z_0.

The corresponding D-H parameters are shown in Table 3-1. Notice that the positive sense for α is determined from z_0 to z_1 if we make a fist with thumbs coincide with x_1 axis by right hand. Similarly, the positive sense for θ is determined from x_0 to x_1 if we make a fist with thumbs coincide with z axis by right hand.

Table 3-1 General D-H Parameter

Parameter Names	Symbols
Joint angle	θ
link twist	α
Link length	a
Link offset	d

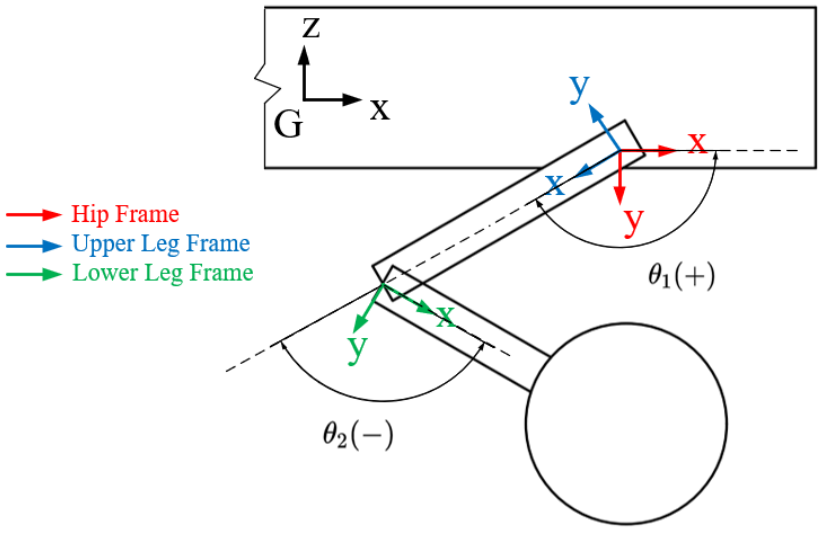

Figure 3-2 D-H frames on FR side

The leg of wheel-legged vehicle can be treated as a planar assembly, so their coordinates satisfy both assumptions of D-H convention automatically if we set the origin at anywhere on the center axis of upper and lower legs. Like shown in Figure 3-2 ,take the front-right leg as an example to set proper D-H frames in the wheel-legged vehicle. The z axes are all neglected in hip, upper leg, and lower leg frames since they can be treated as a planar assembly and the direction of z axis would set automatically by right hand frame rule, and z axis would not affect the motion analysis in local hip frame. θ_1 and θ_2 in Figure 3-2 are defined as 'hip joint angle' and 'knee joint angle' respectively. According to the rules stated in previous paragraph, hip joint angle is a positive value while knee joint angle is negative.

In conclusion, according to the given data in Table 2-1, we can list the D-H parameters of upper leg and lower leg in Table 3-2 and Table 3-3. The initial joint angles are set as empirical values.

Table 3-2 D-H parameters of upper leg

Parameter Names	Symbols	Values
Joint angle	θ	150°
link twist	α	0°
Link length	a	290 mm
Link offset	d	0 mm

Table 3-3 D-H parameters of lower leg

Parameter Names	Symbols	Values
Joint angle	θ	-120°
link twist	α	0°
Link length	a	280 mm
Link offset	d	0 mm

Let's take the FR side as an example again, and the inverse kinematics model can be shown in Figure 3-3 by applying DH convention.

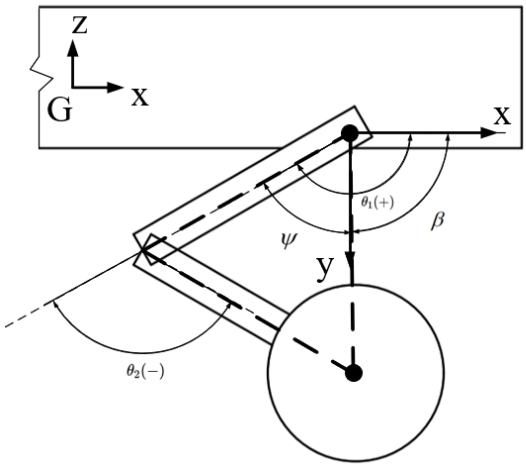

Figure 3-3 Inverse Kinematics Model for FR leg

As stated before, according to the regulations of DH convention, the hip joint angle, θ_1, is in positive domain and the knee joint angle, θ_2 is a negative angle. Since the solutions for inverse kinematics problems are often multiple. For example, a symmetric configuration of links can often achieve the same effect. Because of that, we should define a rational domain of both angles to limit the extreme position of the wheel-legged vehicle. The domain is shown in Equation (3-1), noted that we usually express the magnitude of angles in radians for convenience.

$$\begin{aligned} \theta_1 &\in (\frac{\pi}{2}, \pi) \\ \theta_2 &\in (-\pi, 0) \end{aligned} \tag{3-1}$$

One the one hand, when the hip joint angle reaches its left limit, $\frac{\pi}{2}$, and the knee joint angle reaches its right limit, 0, at the same time, the upper leg and lower leg would be colinear and the vehicle can reach the highest attitude. One the other hand, when the hip joint angle reaches its right limit, π, and the knee joint angle reaches its left limit, $-\pi$, at

the same time, the vehicle is in its lowest position and shows a crawling posture.

In general, there are two different ways to solve for the inverse kinematics problem, geometric method and algebraic method.[30]

3.2 Geometric Method

According to the simple geometric relationships and use the cosine law, we can easily get the expressions of knee joint angle.

$$cos\theta_2 = \frac{x^2 + y^2 - (l_1^{\,2} + l_2^{\,2})}{2l_1 l_2} \tag{3-2}$$

Apply the properties of trigonometric functions, we can get the expressions for $\sin\theta_2$.

$$sin\theta_2 = \pm\sqrt{1 - cos^2\theta_2} \tag{3-3}$$

The parameters that Equation (3-2) contains are all known, so the value of sine and cosine are simple to calculate, then we can apply a useful function $atan2$ to get the final result of knee angle.

$$\theta_2 = -atan2(sin\theta_2, cos\theta_2) \tag{3-4}$$

The $atan2$ function is different from a traditional tangent function in many aspects. The full name of this function is called 'Four Quadrant Inverse Tangent'. It returns values in the closed interval $[-\pi, \pi]$ as shown in Figure 3-4. Moreover, to make the solution lies in the rational domain of θ_2, we choose the positive sign in the expression of sine value and add a negative sign in the $atan2$ function to obey the DH convention.

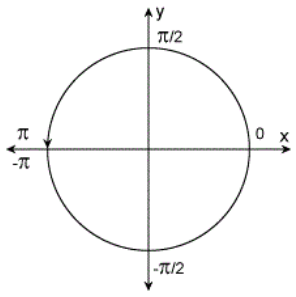

Figure 3-4 The property of atan2 function

After known the value of knee joint angle, we can use advanced graphic method to get the magnitude of hip joint angle. Two auxiliary angles, ψ and β are shown in Figure 3-3. The axis the upper leg and the line connecting hip joint center and wheel center, which is also the direction of leg vector, forms ψ, and the x axis and leg vector forms β. The sum of those auxiliary angles equals hip joint angle like shown below.

$$\theta_1 = \beta + \psi \tag{3-5}$$

The magnitude of β is actually a known value, because the coordinate of wheel center (x, y) is given, and we can apply Equation (3-6) to solve for it.

$$\beta = atan2(y, x) \tag{3-6}$$

Next, to solve for θ_1, we are only supposed to solve for the unknown angle, ψ. The triangle formed by three dashed lines in Figure 3-3 gives inspiration. We can apply sine law in this triangle.

$$\frac{l_2}{sin\psi} = \frac{l_1}{sin(\theta_2 - \psi)} \tag{3-7}$$

Substitute the expression for θ_2, which refers to Equation (3-4), into Equation (3-7), and we can get the tangent value of ψ, finally, the value of ψ.

$$tan\psi = \frac{l_2 sin\theta_2}{l_1 + l_2 cos\theta_2} \tag{3-8}$$

$$\psi = atan2(l_2 sin\theta_2, l_1 + l_2 cos\theta_2) \tag{3-9}$$

Finally, combine Equation (3-6) and Equation (3-9), we can get the ultimate expression of hip angle.

$$\theta_1 = atan2(y, x) + atan2(l_2 sin\theta_2, l_1 + l_2 cos\theta_2) \tag{3-10}$$

3.3 Algebraic Method

The main principle of algebraic method is making use of homogenous transformation matrix to represent that rotation motion occurred at hip joint and knee joint, which are

denoted by H_{knee}^{hip}, H_{wheel}^{knee}, respectively. According to the basic knowledge introduced in Section 2.4, a homogenous matrix is composed by a ration matrix and a translation vector. Check on the DH parameters in Table 3-2 and Table 3-3, we can obtain the homogenous matrix separately for the hip-to-knee transform, and knee-to-wheel transform.

$$H_{knee}^{hip} = \begin{bmatrix} \mathbf{R} & \mathbf{d} \\ \mathbf{o} & 1 \end{bmatrix} = \begin{bmatrix} c_1 & -s_1 & 0 & l_1 c_1 \\ s_1 & c_1 & 0 & l_1 s_1 \\ 0 & 0 & 1 & 0 \\ 0 & 0 & 0 & 1 \end{bmatrix} \tag{3-11}$$

$$H_{wheel}^{knee} = \begin{bmatrix} \mathbf{R} & \mathbf{d} \\ \mathbf{o} & 1 \end{bmatrix} = \begin{bmatrix} c_2 & -s_2 & 0 & l_2 c_2 \\ s_2 & c_2 & 0 & l_2 s_2 \\ 0 & 0 & 1 & 0 \\ 0 & 0 & 0 & 1 \end{bmatrix} \tag{3-12}$$

A continuous transform can therefore be represented by the dot product of Equation (3-11), and Equation (3-12), which generates the homogenous transform from hip joint to wheel center. Moreover, we often use c_{12} and s_{12} to serve as a shortening of $\cos(\theta_1 + \theta_2)$ and $\sin(\theta_1 + \theta_2)$.

$$H_{wheel}^{hip} = H_{knee}^{hip} H_{wheel}^{knee} = \begin{bmatrix} c_{12} & -s_{12} & 0 & l_1 c_1 + l_2 c_{12} \\ s_{12} & c_{12} & 0 & l_1 s_1 + l_2 s_{12} \\ 0 & 0 & 1 & 0 \\ 0 & 0 & 0 & 1 \end{bmatrix} \tag{3-13}$$

On the contrast, we can write the homogenous transform matrix from hip joint to wheel center directly by assuming an unknown angle, ϕ.

$$H_{wheel}^{hip} = \begin{bmatrix} c_\phi & -s_\phi & 0 & x \\ s_\phi & c_\phi & 0 & y \\ 0 & 0 & 1 & 0 \\ 0 & 0 & 0 & 1 \end{bmatrix} \tag{3-14}$$

Since Equation (3-13) and Equation (3-14) show the same homogenous transformation, we can obtain four non-linear equations, from Equation (3-15) to Equation

(3-18), by equating those two matrices.

$$c_{\phi} = c_{12} \tag{3-15}$$

$$s_{\phi} = s_{12} \tag{3-16}$$

$$x = l_1 c_1 + l_2 c_{12} \tag{3-17}$$

$$y = l_1 s_1 + l_2 s_{12} \tag{3-18}$$

Next step is to solve this equation system by algebraic approach. Add the square of Equation (3-17) and (3-18) together, and use basic associativity property of trigonometric functions shown in Equation (3-19), we can get Equation (3-20).

$$\begin{aligned} c_{12} &= c_1 c_2 - s_1 s_2 \\ s_{12} &= c_1 s_2 + s_1 c_2 \end{aligned} \tag{3-19}$$

$$x^2 + y^2 = l_1^2 + l_2^2 + 2 l_1 l_2 c_2 \tag{3-20}$$

It is astonishing to find that Equation (3-20) depicts the same relationship that has already been shown in Equation (3-2). That means the algebraic and geometric method give the same result of knee joint angle. Apply similar analyze process in Section 3.2, the magnitude of knee joint angle is the same as Equation (3-4). When the knee joint angle is solved, we can rearrange the Equation (3-17) and (3-18) to treat the coefficients that contains the trigonometric function of θ_2 as known values. After rearrangement, new equations are shown below, where the coefficient k_1 is the substitution of $l_1 + l_2 c_2$, and k_2 is the substitution of $l_2 s_2$.

$$x = k_1 c_1 - k_2 s_1 \tag{3-21}$$

$$y = k_1 s_1 + k_2 c_1 \tag{3-22}$$

Apply the coefficient substitution method again, let's use r and γ to substitute the coefficient to rearrange the equations above into a more simple and pleasant format as shown in Equation (3-24).

$$\begin{aligned} r &= \sqrt{k_1^2 + k_2^2} \\ \gamma &= tan^{-1}(\frac{k_2}{k_1}) = -\operatorname{atan}2(k_2, k_1) \end{aligned} \tag{3-23}$$

$$\begin{aligned} \frac{x}{r} &= \cos\gamma\cos\theta_1 - \sin\gamma\sin\theta_1 = cos(\gamma + \theta_1) \\ \frac{y}{r} &= \cos\gamma\sin\theta_1 + \sin\gamma\cos\theta_1 = sin(\gamma + \theta_1) \end{aligned} \tag{3-24}$$

Use the 'Four Quadrant Inverse Tangent' function again, we can easily get $\gamma + \theta_1$.

$$\gamma + \theta_1 = \operatorname{atan}2\left(\frac{y}{r}, \frac{x}{r}\right) = \operatorname{atan}2(y, x) \tag{3-25}$$

$$\theta_1 = \operatorname{atan}2(y, x) + \operatorname{atan}2\left(k_2, k_1\right) \tag{3-26}$$

Finally, we get the angle of hip joint as well by using only algebraic method, and the result can be reverified because Equation (3-26) and Equation (3-10) show the same expression for the hip angle of front leg. When it comes to the rear legs, we can take almost the same method and get the result in the same format.

Chapter 4 Modelling of the Wheel-legged Vehicle

4.1 Dynamic Model of Mass-Spring-Damper System

Considering a classical mass-spring-damper system shown in Figure 4-1, from Wikipedia, the mass of m is constrained to be able to move only vertically, and the lower side of the spring of stiffness k_P is fixed to the ground and a parallel damper with damping coefficient k_D is also a fixed to the ground. The higher side of spring and damper are all free. As usual, omit the mass of spring and damper, which means they will stay on their original position if no external force acting on them.[31]

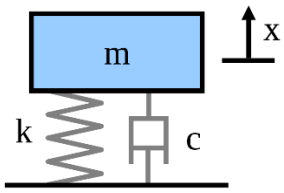

Figure 4-1 Classical mass-spring-damper system (from wiki)

Assume the spring obey Hooke's Law during deformation, which means it is a linear spring that satisfy the Equation (4-1).

$$F_{spring} = k_P x \tag{4-1}$$

Assume the damper is a linear damper, which means the viscous force is proportional to the velocity as shown in Equation (4-2).

$$F_{damper} = k_D \dot{x} \tag{4-2}$$

Consider the free vibration case for the mass, with zero initial position and zero initial velocity. According to the Newton Second Law, the dynamic equation of the mass can be written as below.

$$m\ddot{x} + k_D \dot{x} + k_P x = 0 \tag{4-3}$$

4.2 Define Virtual Force

Consider the same mass-spring-damper system in the previous section, the motion and final state of the mass would be the same if the spring and damper were moved and replaced by a virtual force that exert exactly the same force on the mass. That force is so-called virtual force, F.

$$F = -k_D\dot{x} - k_P x \tag{4-4}$$

We can also define different initial state for the spring and damper. Set the initial length of spring as x_d, and initial velocity of damper as $\dot{x}_d$, then the expressions of virtual force can be rewritten as the equation below.

$$F = k_D(\dot{x}_d - \dot{x}) + k_P(x_d - x) \tag{4-5}$$

4.3 Virtual Model Control Model for the Vehicle

The virtual model control method was first applied on bipedal robots successfully. The idea is to first set the corresponding virtual components on the body degrees of freedom that need to be controlled, for example, in two-dimensional space, it is necessary to control three degrees of freedom, the forward speed of the biped robot, the height of the body and the slope angle of the body. The corresponding virtual components are set to construct virtual forces and torques. The global Jacobian matrix maps all virtual forces into the desired torques of the active joints of the support legs, and finally applies the corresponding desired torques in different states to drive the robot to walk in dynamic balance. The specific details of the application of VMC on biped robots can be found in the bibliography[27]. In the same way, we can extend this idea into wheel-legged vehicles with four legs. The desired degrees of freedom to be controlled are forward speed, stand height, roll angle and pitch angle.

By converting the problem that focus on the center of mass to the state of each leg, the problem can be decomposed and decoupling, so let's analyze the four aimed degrees of freedom one by one to see how they can be controlled by virtual models. Note that we always assume the wheel-ground contact points are known and no wheels are suspended.

(1) Stand height: usually there are two common modes to control the stand height of

the body, absolute height and relative height. Absolute height means the vertical distance between a fixed origin point, and relative height means the distance between the current ground in the direction perpendicular the ground. If the ground is long, horizontal and flat, the absolute height and relative height would be the same. We can choose the control mode according to the application. Since the height of COM, z_G, can be determined by the height of front leg (z_f) and rear leg (z_r),by the relationship $z_G = \frac{1}{2}(z_f + z_r)$, the height of COM can be controlled indirectly by the height of front leg and rear leg. We can set virtual springs and virtual damper, in each hip frame to control the height of each leg and thus controlling the height of the body, with free length z_d for the virtual spring and free velocity $\dot{z}_d$ for the virtual damper. Then the virtual force, on one single leg, in vertical direction can be calculated by using the method shown in Equation (4-5).

$$F_z = k_{DZ}(\dot{z}_d - \dot{z}) + k_{PZ}(z_d - z) \tag{4-6}$$

The subscript Z in the formula is used to distinguish the spring stiffness and damping coefficient in z direction with the structural parameters in x direction. Later, it will show that the structural parameters in different directions can influence the behavior of the system heavily.

(2) Forward speed: Actually, the vehicle can only be driven by four wheels that contact with the ground, so changing the rotation speed of the wheel would change forward speed of the body. However, the body has the degree of freedom to move forward and backward with respect to wheels, which means the velocity and acceleration of wheels can not represent the state of the body directly since the DOF of hip joints. What directly influence the forward speed of the body is the forward speed of the origins of hip frames. We can still set virtual springs and virtual dampers, with free length x_d for the virtual spring and free velocity $\dot{x}_d$ for the virtual damper, to control the forward speed of the body to match the rotation speed of wheels. Then the virtual force, on one single leg, in forward direction can be calculated by using the method shown in Equation (4-5).

$$F_X = k_{DX}(\dot{x}_d - \dot{x}) + k_{PX}(x_d - x) \tag{4-7}$$

(3) Roll angle and pitch angle: we don't need extra virtual components to control the roll angle and pitch angle because the height of front leg and rear leg can also determine the posture angles of the body. The exact relationship between posture angles and height of legs has been descripted in the posture analysis chapter. To measure the current posture of the body, many vehicles would use inertial measurement unit (IMU) to feedback the current state of the body and then adjust the posture according to the feedback data.

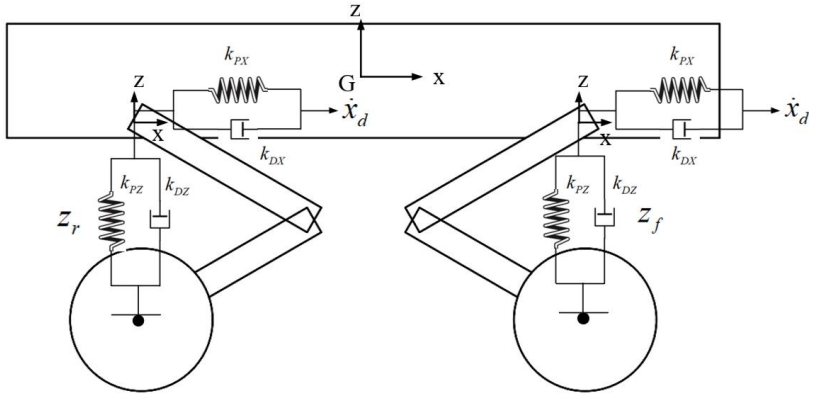

Figure 4-2 Planar Virtual Model of the Wheel-legged vehicle

Once the virtual forces are set up, we should figure out the relationship between the force and the joint torque, because the joint torque is the only value that we can easily controlled by controlling the motor. The position relationship between the joint angles and the position of the wheel center in hip frame can be analyzed by forward kinematics. According to the geometric relationship, we can get the following equations.

$$\begin{cases} x = l_1 cos\theta_1 + l_2 cos\theta_2 \\ z = -(l_1 sin\theta_1 + l_2 sin(\theta_1 + \theta_2)) \end{cases} \tag{4-8}$$

Take partial differential for the two equations contained in Equation (4-8), we can get the representation of Jacobian Matrix.[32]

$$J = \begin{bmatrix} \frac{\partial x}{\partial \theta_1} & \frac{\partial x}{\partial \theta_2} \\ \frac{\partial z}{\partial \theta_1} & \frac{\partial z}{\partial \theta_2} \end{bmatrix} \tag{4-9}$$

Then the desired torque for each joint can be calculated by Equation (4-10).

$$\tau = J^T F \tag{4-10}$$

Chapter 5 Attitude Simulation for Wheel-legged Vehicle

5.1 Introduction to Simscape Environment

As we all know, when simulating in Simulink, we should build the equations, either differential equations or Laplace form, and then use those equations to represent the physical properties of the plant, and then put it into the block diagram. Simscape is a toolkit embedded in Simulink environment, which means we can composite any methods we are familiar with in a basic Simulink project with the pictorial form in Simscape. It uses different blocks to represent many useful physical components like electric motor, fluid, simple brick solids, or even multibody. Simscape makes the modeling and simulation process more vividly and more efficient instead of deriving every basic differential equation. For example, a basic mass-spring-damper system can definitely be simulated by Simulink because we can use 'Gain' block to represent the parameters and use 'integrator' block to model the properties of spring and damper, like shown in the left side of Figure 5-1. On the contrast, Simscape has integrated all the basic properties of this basic physical system and just show the block as it looks like in real world, or say in a schematic way shown in the right side of Figure 5-1.

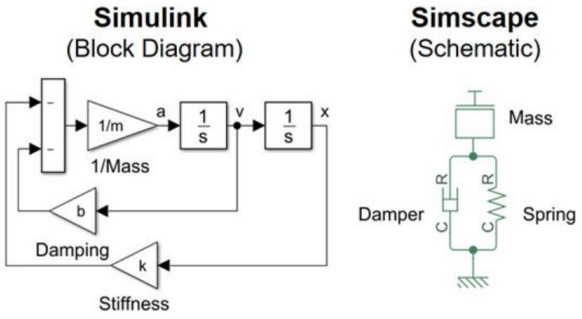

Figure 5-1 Build Simscape Model Easily (Sketch from Simscape Introduction Pages)

By simply double click, researchers can adjust every essential parameter that influence the system. And just like what to do in Simulink, we can build a composite system by simply linking every subsystem. It is a more intuitive way to build and to show the model of the

system. Generally speaking, Simscape includes 'Power System', 'Multibody', 'Simscape Fluid', 'Simscape Driveline', and 'Simscape Electronics'.

5.2 Set a Simscape Model

The whole wheel-legged vehicle should be split into lots of small components, including body, upper legs, lower legs, and wheels. Since the project does not contain the mechanical structure and control of electric motor, there is no need to build a motor part. We should set up appropriate 'joint' between each component to link them. Setting convenient coordinates in Simscape is also of vital importance. Each Simscape model contains a 'world frame', which is a fixed built-in frame, and usually, the software would build a default frame for each solid at the center of mass. Thanks to 'rigid transform' part, we can set the spatial relationship between all the frames according to our own thoughts. Moreover, the Matlab '.m' file can be used to define some parameters to build a parametric workflow. Before the start, 'Mechanism Configuration' should be properly set up, which includes the direction and dimension of uniform gravity. In this project, the gravity is set to be along $-z$ direction with acceleration of $-9.80665\ \mathrm{m/s^2}$. In the following, the process to build a basic wheel-legged vehicle is going to be briefly introduced.

5.2.1 Physical Model

Locating the Vehicle Body and Ground: A 'brick solid' part is applied to represent the geometry of the vehicle body, which is a simple cuboid, with the mass of 60kg, which refers to the total mass of body and load that given in the specification. The vehicle body is directly attached to the world frame by a 'Bushing Joint', which is actually a combination of three prismatic joints, providing three translation degrees of freedom, and three revolute joints, providing three rotation degrees of freedom. That makes sense because in real world, the body is a free part if there is no leg to support it, which also means the body is a passive component and there is no need to define a drive force for it in Simscape as well. The simple ground is a long flat solid that attached to the world frame directly with a displacement in vertical direction.

Set upper legs: A long lever is generated by 'brick solid' with the length of 290mm,

according to the specification. To set four upper legs properly, we should use 'rigid transform' part again to locate the position and orientation of four hip frames. The upper leg is articulated with the body, so 'revolute joint' is suitable to constrain the hip joint. By setting initial state of the revolute joint, we can control the initial stand attitude of the vehicle. It is worth mentioned here that, since Simscape stipulates that the revolute joint can only rotate along its z axis, so the z axis of the actual hip frame are perpendicular to the z axis of world frame. In physical model, there must be an electric motor mounted at the hip frame to control the angle or torque actively. Similarly, the 'revolute joint' in Simscape can be driven by two kinds of signal, angle or torque.

Set lower legs: Lower legs are articulated with the upper legs and wheels. Similar to the set up of upper legs, the 'revolute joints' are set up at the end of lower legs, so as the other end, and the length is set to be 280mm.

Set the wheels: Use the 'Cylindrical solid' to represent the geometry of wheels. There are also revolute joints at the center of wheels to simulate the wheel axis and wheel-side actuator. Since the treads of wheels are the only contact surface with the ground in the model to support the vehicle, we should first extend the geometry of wheels and ground to simulate the contact forces by using the 'Spatial Contact Force' block, which can apply contact force between a pair of attached components. This block simulates the force in conformance with Newton's Third Law, including normal force and friction force. To make the simulation more accurate, we should set several coefficients that related to normal and friction force, appropriately. Table 5-1 shows the value of every important coefficient that influence the contact behavior.

Table 5-1 Coefficients of Contact Force

Types of forces	Coefficients	Values
Normal Force	Contact Stiffness	1×10^{6} N/m
	Contact Damping	1×10^{4} N/(m/s)
	Contact Transition Region	1×10^{-4} m
Friction Force	Static Friction	0.9
	Dynamic Friction	0.89
	Critical Velocity	1×10^{-2} m/s

5.2.2 Matlab Function Block in Simscape

'Matlab Function' block is a useful embedded part in Simulink, that allows user-defined function to link to other parts in Simulink. It simplifies the whole system with convenient input/output ports and we can simply link the ports with other blocks in Simulink. However, the Simscape environment is defined to be a physical environment that is different from Simulink environment. Any data created in Simulink cannot be transmitted directly into physical Simscape block unless through a 'Simulink to PS converter'. The 'converter' block should be appropriately set to ensure the units or derivatives are correct.

Based on the method introduced in Section 2.5, a Matlab Function block called 'Cal_Leg_Vector' is built to calculate four leg vectors at the same time. As shown in left part of Figure 5-2, there are several input ports to set up the initial configuration of the vehicle, including the translation of hip frames relative to frames at the center of mass, desired posture angles, initial stand height and so on. The output ports only contain the planar coordinates of wheel centers in hip joint frames, which also means the leg vectors. The output data of 'Cal_Leg_Vector' function is directly input to another function called 'Inverse_Kinematics' which is responsible to calculate joint angles according to the input vectors. The output ports are targeted angles of joints on each side.

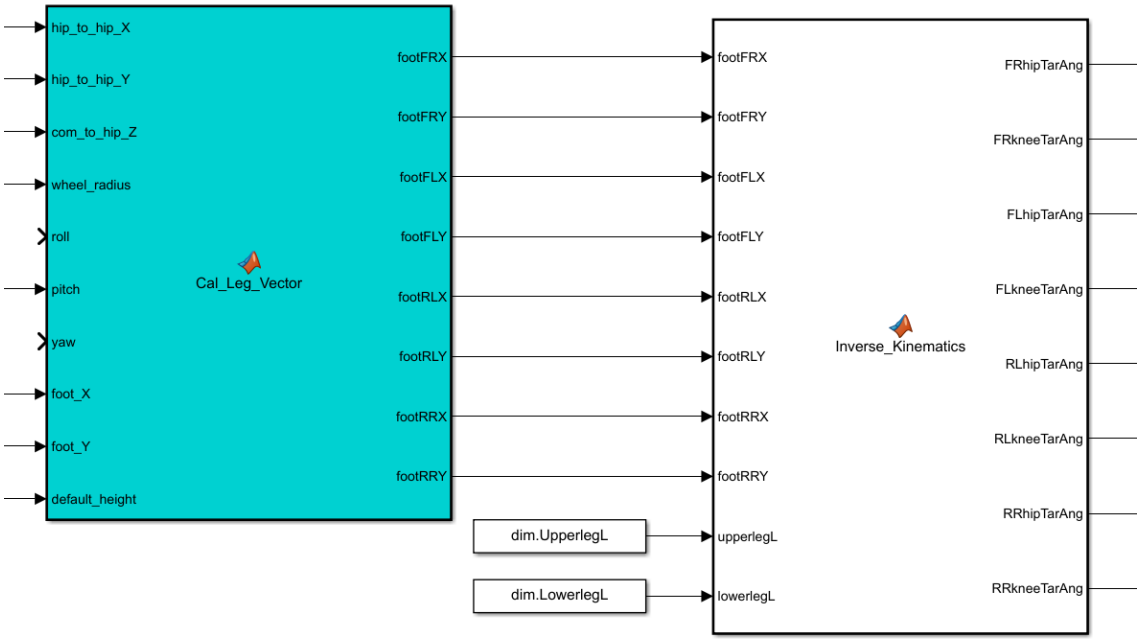

Figure 5-2 Matlab Functions

5.2.3 Test the Basic Physical Model

Define the motion of each 'Revolute Joint' is provided by input and the torque is automatically computed, which means we only control the angle of the joint, other than controlling the torque. In such circumstances, the output of those two functions in Figure 5-2 can be directly handed out to every hip and knee joint to control the attitude of the wheel-legged vehicle by pure position-control. If all the bodies are correctly set up as stated before, the basic wheel-legged vehicle will show on the screen as shown in Figure 5-3, with zero initial pitch angle and zero initial roll angle. Different types of components are painted with different striking colors to make it easy to distinguish them.

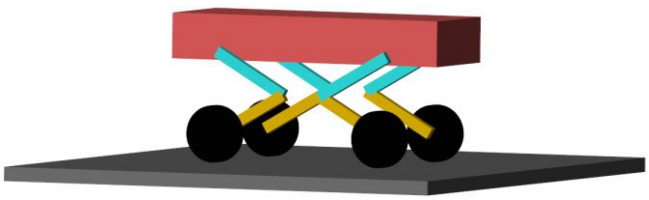

Figure 5-3 Basic Multibody Physical Model

To test the accuracy of leg vector calculation part and inverse kinematics part, we can measure the pitch angle, roll angle and stand height of the body by the 'sensing' function of 'Bushing Joint' as shown in Figure 5-4. There are also sensing function at 'revolute joint', that serve as hip joint, knee joint and wheel joint.

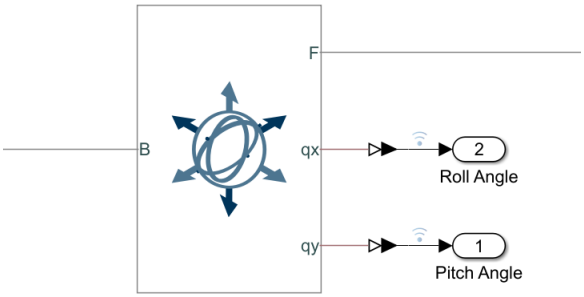

Figure 5-4 the 'sensing' function of 'Bushing Joint'

Use the 'Signal Builder' block, we can generate any basic signals to play a role as desired angles. The test signal, with a total timespan of 12 seconds, has been built through such approach. It remains zero for 2 seconds at the beginning, and then take a ramp increase to 10 degrees in 2 seconds, holding constant for another 2 seconds. At the 8 second, the signal begins to decrease linearly for 2 seconds long, and finally remains zero state in 10 seconds to 12 second.

Pitch Test: The whole vehicle is stationary with non-rotating wheels, and desired roll angle is zero. Actuated by the signal described before, the vehicle shows fantastic attitude controllability as shown in Figure 5-5. The solid line in red is the trajectory of desired pitch angle and dashed line in blue with dispersed dots are the actual behavior of the vehicle. It shows that the pitch angle of the vehicle follows the aimed value perfectly without any error or delay. The snapshot of the posture at pitch angle of 10 degree is shown in Figure 5-6. Agreed with the intuition, front legs (including both FR and FL leg) bend, and rear legs (including both RL and RR leg) stretch to lean the body forward.

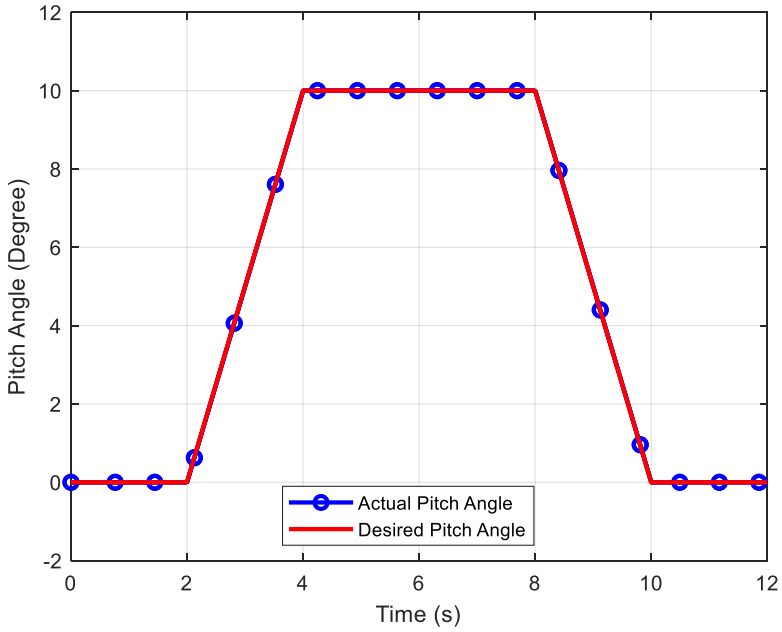

Figure 5-5 Pitch Test

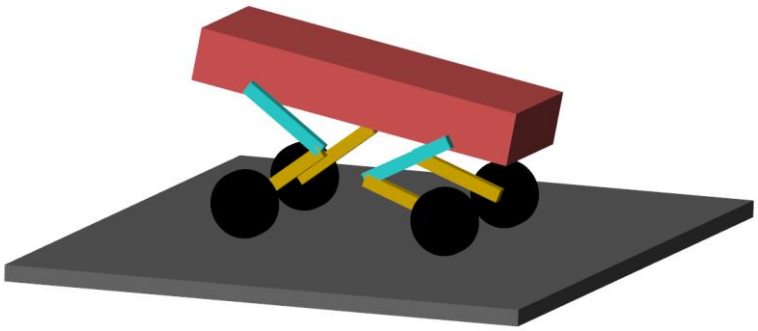

Figure 5-6 Pitch Angle = 10°

Previous testing proves that the method of calculating leg vectors and the inverse kinematics solver are both absolutely correct without any theoretical error. Guided by those functions, each joint is actuated by providing angles, and the angle of every important joint when the pitch angle is 10° are listed in Table 5-2.

Table 5-2 Joint Angles when Pitch = 10°

Location	Hip Joint Angle (Degree)	Knee Joint Angle (Degree)
FR	142.7027	-132.39
FL	142.7027	-132.39
RL	26.0514	106.3955
RR	26.0514	106.3955

Roll Test: Similar to the pitch test, apply the same input signal to the stationary vehicle, and the desired pitch angle is zero. The behavior of the vehicle is the same as shown in Figure 5-5, there is also no error or delay when controlling the roll angle. The snapshot of the posture at roll angle of 10 degree is shown in Figure 5-7.

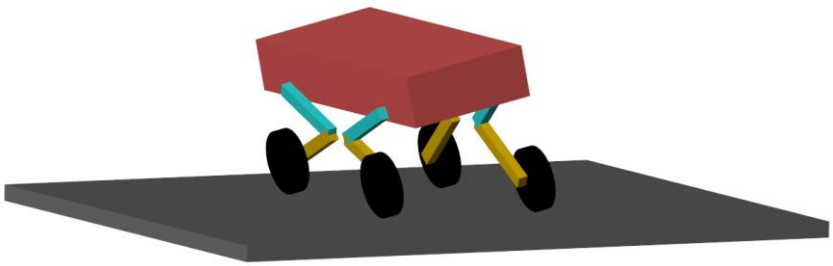

Figure 5-7 Roll Angle = 10°

5.2.4 Build Virtual Model of Legs

Since the 'leg vector' calculation part is the base of 'virtual model' part, we can only build and test the virtual model in Simscape after checking the accuracy of previous function blocks. We use position-control mode of the revolute joint to test 'leg vector calculation' part and 'inverse kinematics' part. On the contrast, the virtual model generates virtual forces and virtual torques as described in Section 4.3. We should change the mode into 'torque control' mode, which means the angle is calculated automatically according to provided torques.

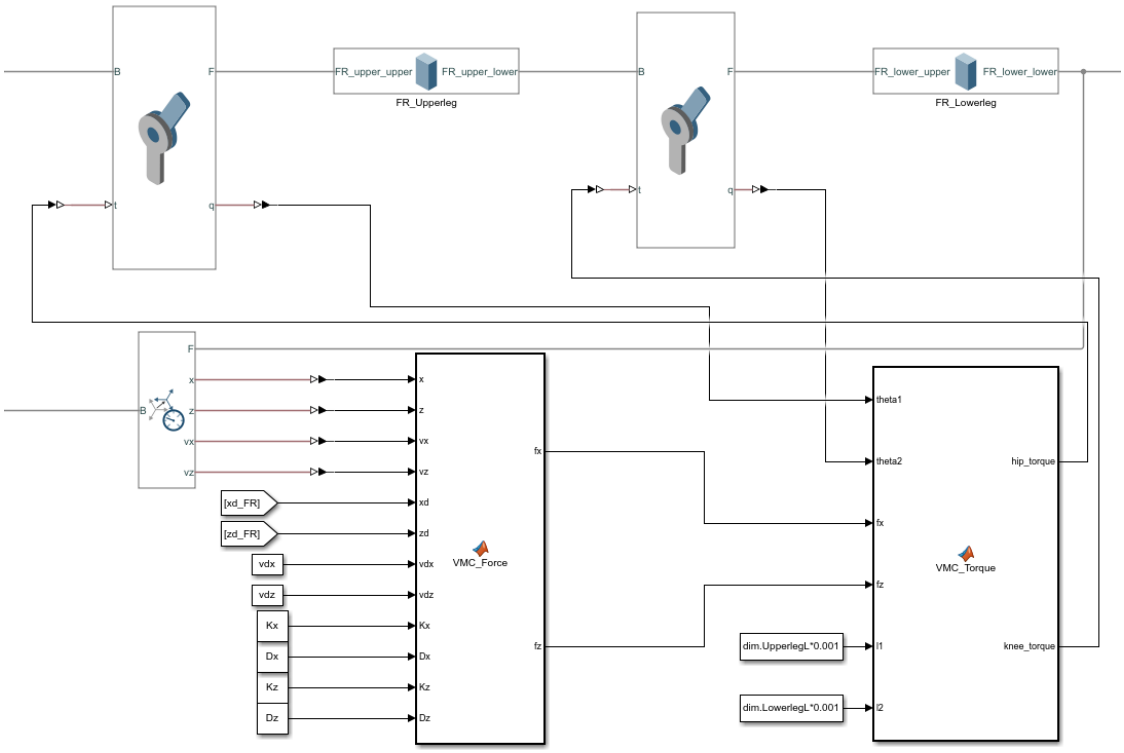

Figure 5-8 Virtual Model of the leg

As shown in Figure 5-8, the 'VMC_Force' function is built to achieve the equation relationships in Equation (4-7), and get the virtual forces in both vertical and forward direction. This function needs several essential input data, collected from the 'sensing' function of joints and 'Transform Sensor' block of Simscape, and desired position, and velocity in both directions. The desired value is provided by 'leg vector' calculation part. Since we need the current angle of hip and knee joint in Jacobian matrix, we should collect those data from the revolute joint blocks and send them into the 'VMC_Torque' function, which derives the torque directly by calculation Jacobian matrix simultaneously. The magnitude of torques are sent as actuation signal for hip joints and knee joints.

Since the dynamic performance of the virtual spring-damper system is highly related to the mass, we usually treat the upper leg and lower leg as light levers, which means omitting the mass of legs. In that the wheels always contact with ground, the mass of wheels would not affect the behavior of the virtual model system. In summary, we set the total mass

of the body as the sum of body mass, m_B, and load mass, m_L, which refers to 60kg. Each wheel is set to weights 2.5kg.

5.3 Tuning the Parameters of Virtual Model

The spring stiffness and damping coefficient should be well tuned to make the leg stiff enough to support the body and the leg should be soft enough to absorb external shock exerted on wheels. The performance of the vehicle at the moment it touches the ground after a free falling-down process is an important evaluation method to show the softness and hardness of the leg in vertical direction. To tune the coefficient in forward direction, we can examine a uniform acceleration condition.

5.3.1 Parameters Tuning in Vertical Direction

The vehicle is lifted beyond the ground and then it falls freely under the influence of gravity force. Initially, the vehicle holds its default stand height, $335mm$. Since, by now, no controller is applied, the legs of the vehicle will behave only according to the virtual model parameters, K_{DZ} and K_{PZ}.

Figure 5-9 shows the oscillation performance of stand height in vertical direction with different coefficients of damping, K_{DZ}. With the same spring stiffness, K_{PZ}, it is shown that the system with lowest damping coefficient reacts far more quickly than others, but the overshoot is also much greater than others', which is not a desired response. The system with larger damping coefficient behaves more stable with less settling time, just like the green line in the figure. If the overshoot is too large, the vehicle will bump severely when contacting the ground for a long time. There is also a common property for all the systems, that steady-state error. The desired stand height of the vehicle is $335mm$, but all the tuned systems shown in Figure 5-9 reach steady position at the height of $190.5mm$. A large steady state error exists for the system, and it shows the stiffness of virtual spring influence the steady-state error directly.

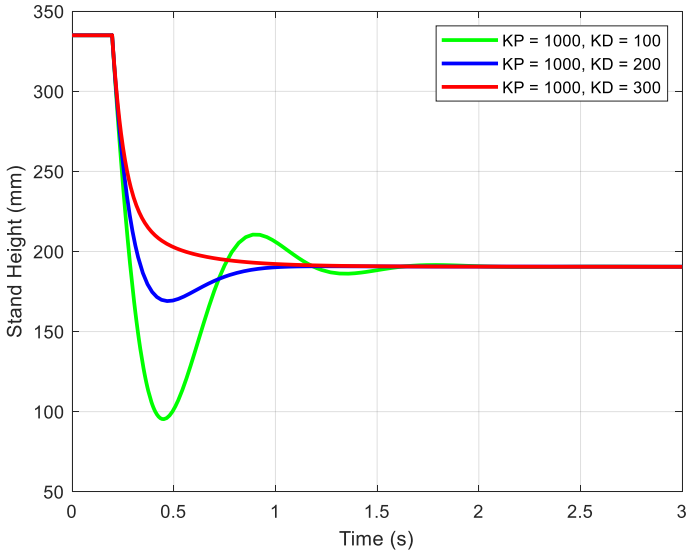

Figure 5-9 Performance of Stand Height with Different Damping Coefficients

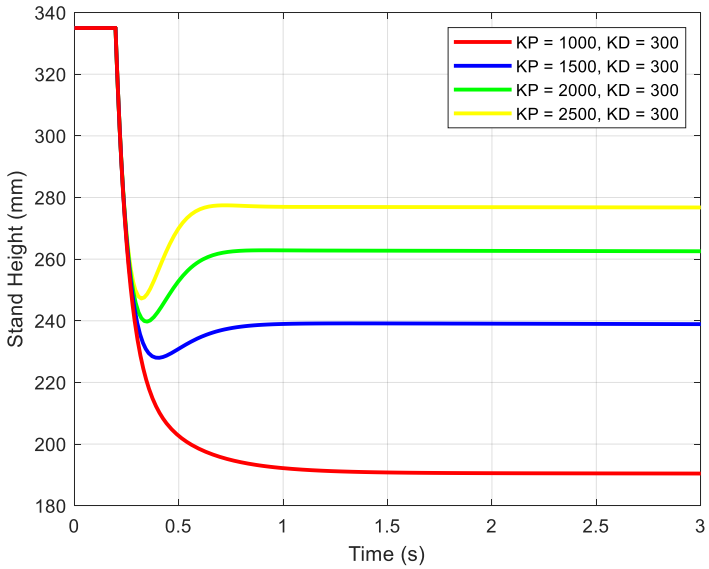

Figure 5-10 Performance of Stand Height with Different Damping Coefficients

As shown in Figure 5-10, the stand height at steady state increases as K_{PZ} increases. That makes sense, because softer spring cannot support the load unless undergoing larger deformation. However, as the spring stiffness increasing, peak time shifts forward with larger overshoot. Since those systems have the same damping coefficient, that response

speeds at the beginning are the same.

In brief conclusion, increase the stiffness of virtual spring can reduce steady-state error, but with larger overshoot. Increase the damping coefficient of virtual damper can increase the response speed at the beginning and can inhibit overshooting effectively. Both coefficients should be matched perfectly to build a stable and beautiful system.

5.3.2 Parameters Tuning in Forward Direction

As stated in Section 4.3, the forward speed of the body is controlled by the horizontal virtual spring and damper, so the coefficients affect the behavior the body in horizontal direction. During the parameter tuning process, I found that if K_{PX} and K_{DX} are too small, the motion of the body would lag behind wheels. That circumstance is serious in acceleration state.

Figure 5-11 shows the 'lag' posture of the body. When accelerating, the body cannot catch the speed of wheels, and wheels are not located directly below the body, which means the center of contact plane leads the center of mass.

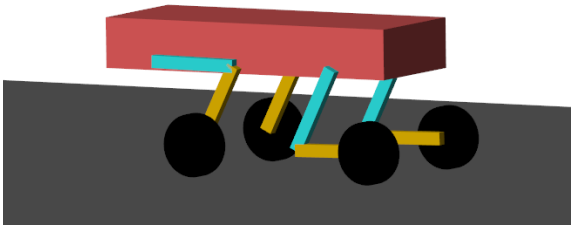

Figure 5-11 Body lags behind wheels

Let wheels accelerate at the time of 1 second, and keep uniform acceleration until 2.5 seconds. The red line in Figure 5-12 shows the linear velocity of wheel center in forward direction, other lines shows the velocity response of the center of mass on body. It shows that, with the same spring stiffness, smaller damping coefficient causes severe oscillation, which means the body will toggle the modes from 'lag' to 'lead' again and again. The oscillation in the center of mass is not desired, and bas smoothness can cause damage if the

wheel-legged vehicle is applied in factory or battlefields.

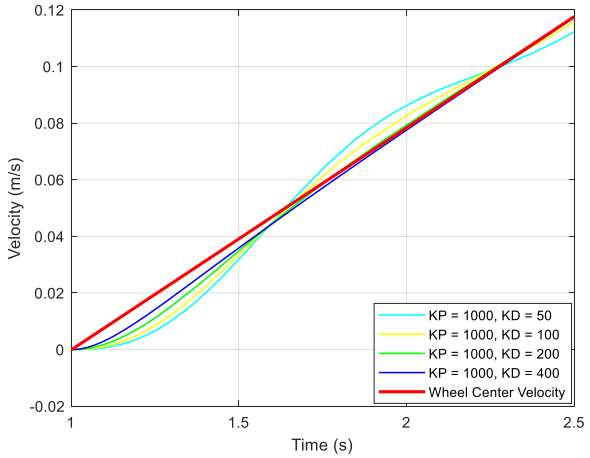

Figure 5-12 Compare COM velocity with wheel speed during acceleration

5.3.3 Determine Parameters According to Torque limits

The content in previous sections show that the vertical and horizontal virtual components determine the dynamic performance of the body together. In that the magnitude of virtual force is proportional to spring stiffness and damping coefficient, we should set coefficient thresholds to limit the assigned torque on each joint motor. Specifically, the maximum torque of hip joint and knee joint should not exceed $150Nm$, and the maximum torque of wheel joint should not be greater than $27Nm$ according to the given data in Table 2-1 Wheel-Legged Vehicle Specification.

Finally, the spring stiffness and damping coefficient are determined by considering all the elements described before, including bumping performance, support stiffness, torque limit and so on. The exact values are shown in the table below. The spring stiffness in vertical direction is set be stronger than in horizontal direction, because usually the attack to vehicle is in vertical direction by undulation of terrains. Moreover, the acceleration in forward direction is often much smaller than that in vertical direction. Correct damping values are here to diminish undesired oscillation and to prevent large overshoot.

Table 5-3 Final Value of the Coefficients of Virtual Components

Symbols of Parameters	Values
k_{PX}	3000
k_{DX}	400
k_{PZ}	5000
k_{DZ}	1500

The rationality of this set of parameters is to be proved by passing through Terrain 1 (Figure 5-13 Terrain 1: Terrain with scattered obstacles), which is formed by irregular scattered obstacles, and the corresponding hip joint torque and knee joint torque are shown Figure 5-14.

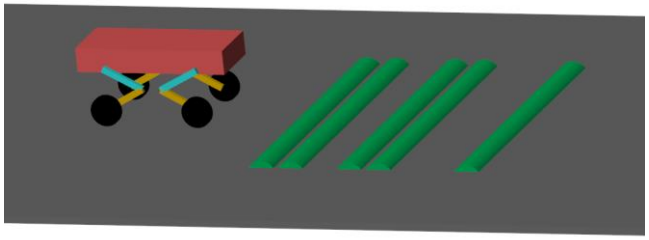

Figure 5-13 Terrain 1: Terrain with scattered obstacles

The maximum torque of hip joint torque is around $-40Nm$, and the ones of knee joint is around $100Nm$. The peak value occurs when contacting with obstacles. The peak value of both hip joint and knee joint are below the limit of joint motors, which refers to $150Nm$, according to Table 2-1. At normal state when no external attack occurs, the support torque of hip joint and knee joint are all lower than the given continuous torque of the motor, thus showing that the magnitude of spring stiffness and damping coefficient are rational. Moreover, the knee joint is often responsible for absorbing more external impact, which can

be easily observed from Figure 5-14. That meets the principle of bionics, because the knee joints of our human beings are usually more easily to be worn than hip joint, and knee joint exerts much larger force when we do actions like jumps or squat.

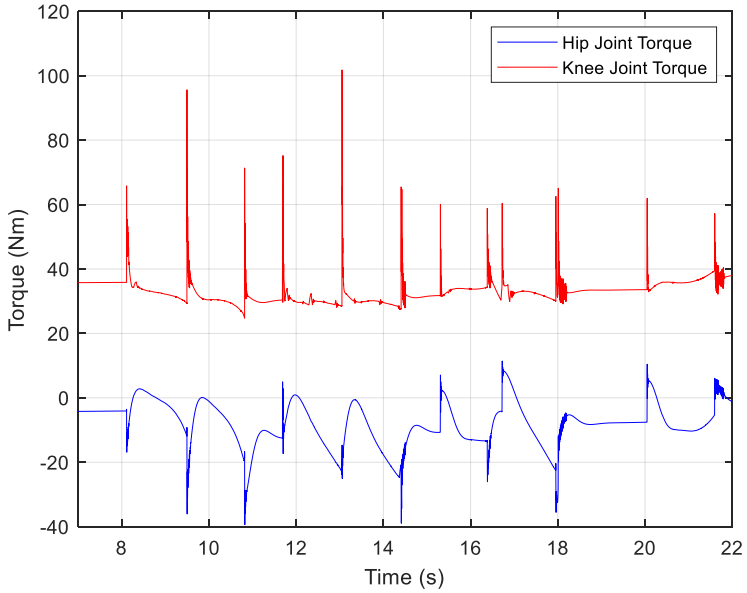

Figure 5-14 Joint Torque when passing through obstacles

Chapter 6 Attitude Stability Control Scheme

All the contents in previous chapters, including calculation leg vectors, forward and inverse kinematics and virtual model, serve as the subpart of attitude stability control scheme. The main purpose of the project is to increase the stability of wheel-legged vehicle when crossing tough obstacles, and a closed loop control method is shown in Figure 6-1.

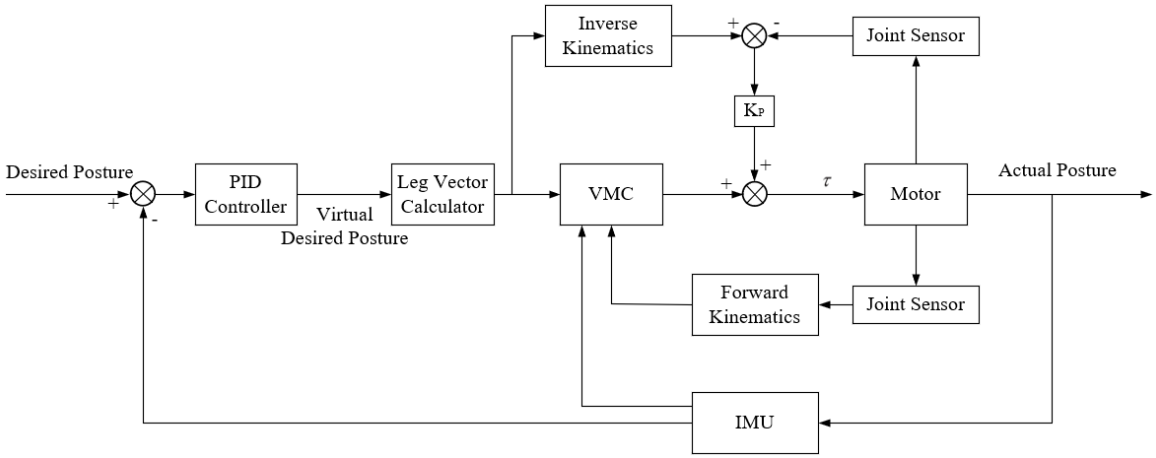

Figure 6-1 Attitude Stability Control Scheme

6.1 General Explanation of the Control Method

The input signal of the whole system is 'desired posture'. Generally, it refers to desired pitch angle, desired roll angle, and desired stand height of the vehicle relative to the frame fixed to a horizontal and flat ground. On the right side, the output signal of the whole system is the attitude of the wheel-legged vehicle. Since open-loop control cannot reach the desired attitude accurately and rapidly, an inertial measurement unit (IMU) is essential. It is mounted at appropriate position of the wheel-legged body to measure the angular position, angular velocity and angular acceleration along each axis. The data collected by IMU can represent the real-time status of the body, and it is served as feedback signal. Summing up the input signal and feedback signal from IMU, a classical proportional–integral–derivative (PID) controller, which will be explained in detail later, is set before 'calculate leg vector' block. This block contains all algorithm shown in Section 2.5, and outputs the wheel

positions of each leg in hip frames, in vector form. In the following path, 'VMC' block take leg vectors as one of the input signals, and process those data according to the virtual model control method explained in Section 4.3.

'VMC' block can be imagined to be separated into two parts, calculating virtual force and calculating virtual torque. The first part can be completed by the input signal from 'leg vector' block and the feedback signal from, still, IMU. Here, IMU feeds back the current forward speed, and vertical velocity and position in both directions. For the second part, it is obvious that 'VMC' block also need to process the real-time feedback of current angular position from the sensors on joint motors, because deriving expression of Jacobian matrix need current angular position, shown in the partial differential operators in Equation (4-9), and also forward kinematics. Sensors integrated in the structure of joint motor are responsible to monitor the current angle of the motor, which are common and cheap sensors compared with expensive torque sensors. Forward kinematics block is also a prerequisites of Jacobian matrix. In totally, 'VMC' block receives data from three different paths, one from the main path, and the other two are from feedback paths.

As for the 'motor' block, it is the final plant in the system driven by torque. The magnitude of torque is the signal that determine the posture of the wheel-legged vehicle. It is not only generated by the output torque of VMC, because the inherent drawbacks of mass-spring-damper system, which means steady-state error. The disadvantages of steady-state error will be descried later. To conquer the disadvantages of steady-state error, 'inverse kinematics' block is mounted at bypath of the control scheme to generate a compensate signal. Still, the difference between current angular position from joint sensor and the desired angles of hip joint and knee joint has been generated. Since Section 5.2.3 has proved the correctness of inverse kinematics algorithm, the desired signal from inverse kinematics is an absolutely correct signal. A proportional feedback block is used to enlarge the difference between desired angles and actual angles. Add up the torque signal from both 'VMC' block and compensate signal from inverse kinematics block, we can generate the torque to drive the motor, and the attitude changes.

6.2 Virtual Desired Posture

'PID' controller block at the beginning of the control path is used to adjust the signal input to the 'Leg Vector Calculator' block. In general, there are two different kinds of requirement for the vehicle. The first one is to fix the body of the vehicle relative to the current ground. In this circumstance, we only need a constant signal input to the system as desired posture other than the signal processed by PID controller, because the leg vector calculation algorithm shown in Chapter 2 is just relative to the current ground. 'VMC' or 'Inverse Kinematics' block would be enough to fix the body to specific desired attitude. However, the state of the vehicle is decided by external road passively, which is not expected in stability-based mission. The application scenarios of such control method are high speed movement, tough terrains and stability dependent task. The second kind of requirement for the vehicle is to hold the body to a specific attitude relative to an arbitrary fixed frame. For instance, when carrying goods or humans, the vehicle is expected to hold the body absolute horizontal. It does not mean being parallel to the current ground but parallel to virtual sea level. To achieve this goal, we can take the negative value of actual posture angles and add the negative value to the input signal, then the 'PID' block is responsible to generate appropriate signal input to the leg vector calculation process. If the desired pitch angle relative to the fixed frame on the horizontal ground is 0 degree, it means the vehicle should always hold the body horizontal to the fixed frame. That is to say, if the vehicle on a tilted road with 10-degree-slope, the 'virtual desired posture' signal input to the 'leg vector calculator' block should be negative 10-degree pitch angle.

However, tough terrains in real world do not always hold a fixed slope, on the contrast, it is irregular, so the feedback signal from IMU cannot be added to the desired signal directly to form 'virtual desired signal'. The 'PID controller' block take the proportional, derivative and integration of the error signal generated by the difference of 'desired posture' and 'actual posture' to create an appropriate 'virtual desired posture' to the 'leg vector calculator' block, which can be vividly explained in the simulation on the sine-wave terrain shown in the following sections.

6.3 Compensate for the Steady-State Error of VMC

There are inherent limitations for virtual model control, relatively large steady-state error. For instance, if the desired position of a simple mass-spring-damper system shown in Figure 4-1 is zero. The final state of the mass cannot reach the origin at all unless the stiffness of the spring is much larger than needed. Too large stiffness would cause severe oscillations of the system and make the whole system unstable. And such limitations of spring-damper system still exist in virtual model control scheme. For example, in some special tasks, we need the vehicle to behave as accurate as possible, like some vision-based task and missile launching mission. Let's considering we need the vehicle 'heads down' for a scale of 10 degrees and hold stationary, which also means the pitch angle is 10 degrees, and the forward speed is zero.

If omitting the compensate path in Figure 6-1, and the input signal of the system is a constant, 10-degree pitch, the performance of the vehicle can be shown in Figure 6-2.

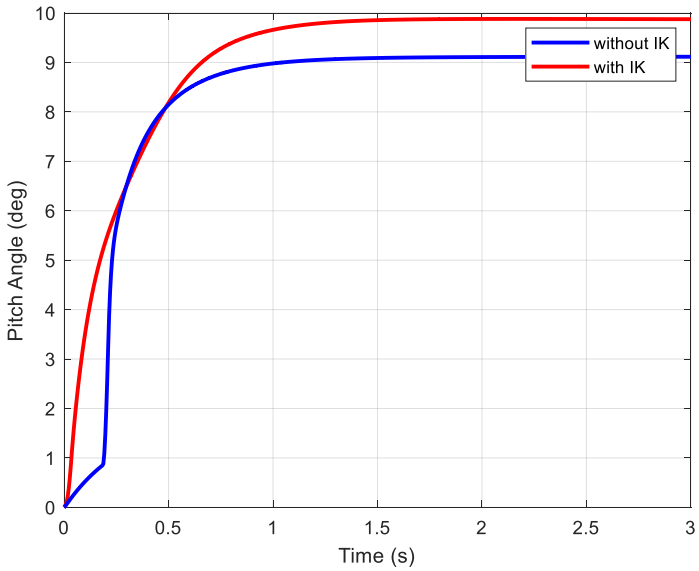

Figure 6-2 Pitch Performance of different control method

The blue solid line in the figure shows that the vehicle can only reach 9-degree-pitch if the input signal is a constant, 10-degree, when the VMC parameters are well tuned. The steady state error is almost 10 percent, which is relatively large than expected. Compensated

by the signal provided by inverse kinematics, red solid line in the figure shows a much better performance with quicker response, less steady-state error and smoother performance. Such phenomenon can be explained by the principle of creating compensate path. If the feedback signal shows that the current joint angle is much lower than the absolute signal provided by inverse kinematics, a positive torque signal generated by scaling up the difference between those two signals is added to the torque signal generated by the 'VMC' block, in that the magnitude of the proportional coefficient, K_P, should also be well tuned to ensure that the compensate signal would not be too large or too small.

Since the whole system is a complex system, and it is hard to derive the theoretical transfer function of the system, so empirical parameter tuning method is practical in this circumstance to tune the coefficients of 'PID' and proportional feedback coefficient, K_P. Finally, a set of rational parameters for the control loop is shown in the table below. (The unit of the input signal before PID block is degree.)

Table 6-1 Coefficients of Controllers

Symbols of Coefficients	Values
P	8
I	10
D	10
K_P	2

6.4 Physic Modeling of Sinewave Terrain

To simulate the attitude stability control scheme stated in previous sections, we need build obstacles on road to simulate tough terrains in Simscape. The 'File Solid' block of Simscape can import solid element along with their geometry structure, inertial, reference frames, colors, materials and so on. It has strong adaptability that can support common computer-aided-design software like CATIA-v5, CATIA-v6, Creo, UG/NX and so on.

Supported file format includes CATPART, PRT, IPT, SLDPRT, X_T, JT, STL, and STEP. In this project, Creo Parametric 8.0 are applied to build the 3D model of terrains, because of its advantages on parametric design. Sinewave can simulate various excitations from road unevenness by adjusting the amplitude and frequency. The geometry of the sinewave can be modelled by the following equations, the unit is millimeter.

$$\begin{cases} x = 400t \\ y = 40\sin(360(t-0.25)) \\ z = 0 \end{cases} \tag{4-11}$$

Input the equations above into the 'Curve from Equations' part in Creo Parametric, and extrude the closed sketch to a solid show in Figure 6-3.

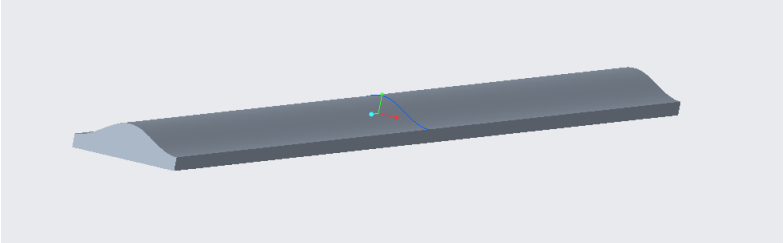

Figure 6-3 3D structure of sinewave terrain in Creo Parametric

The sectional curve of the sinewave road can be shown in Figure 6-4. The peak-to-peak value is 80 mm, which is around the wheel radius of the vehicle. Obstacles near wheel-radius size are the most common terrains during application.

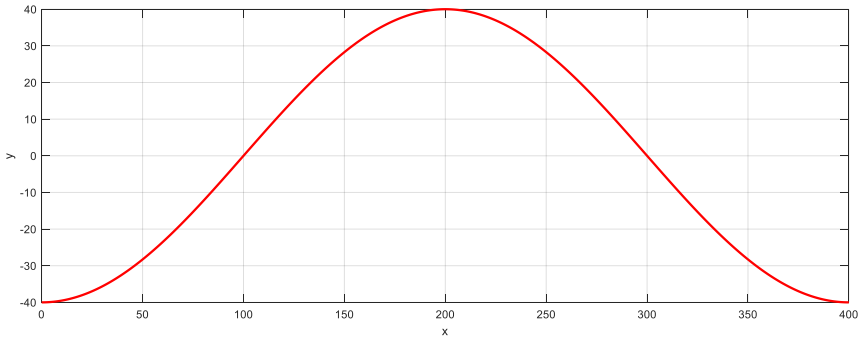

Figure 6-4 Geometry of the Sectional Curve of Sinewave Terrain

6.5 Single Aim Verification on Terrain 2 (Pitch Angle Test)

To test how the pitch angle of vehicle performs when crossing obstacles that are symmetric at both side of $+x$ axis. Put five such terrains together to form a consequent unevenness terrain to test the dynamic behavior of the vehicle when crossing continuous obstacles, which is shown in Figure 6-5. The terrain 2 is set to be symmetric at left and right side of the vehicle to avoid rolling in lateral direction, which could influence the pitch performance.

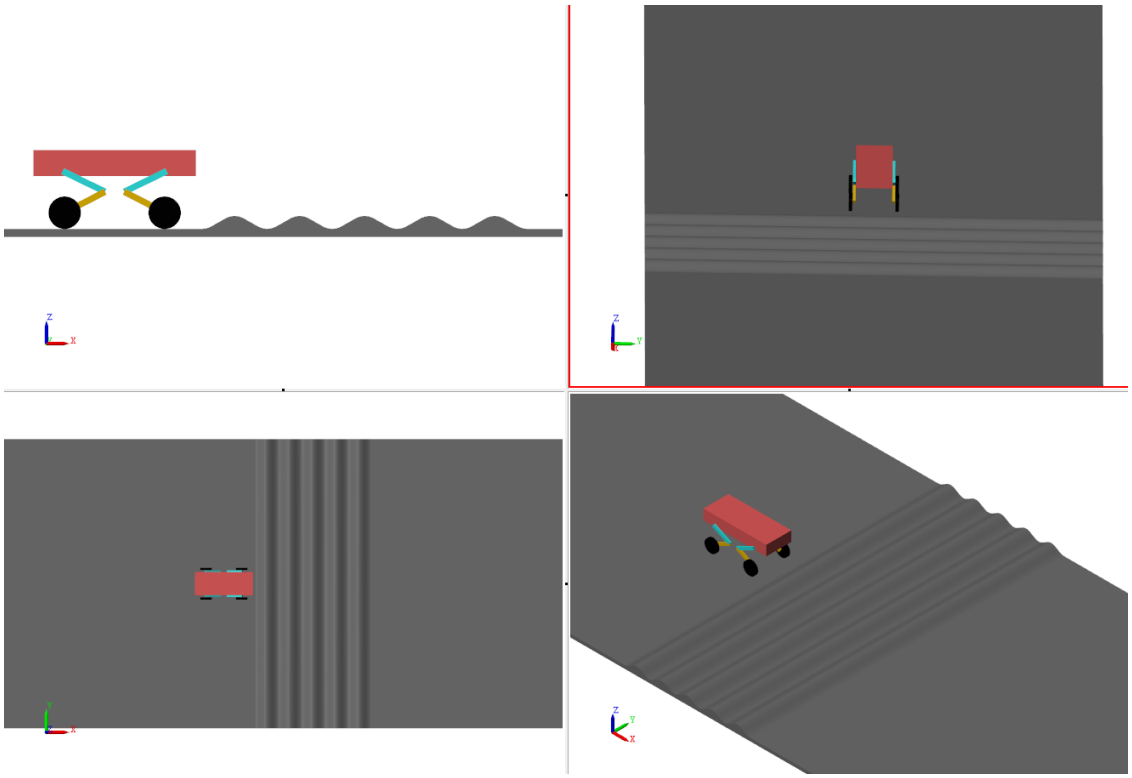

Figure 6-5 Terrain 2: Pitch Test

For this experiment, the desired pitch angle of the vehicle is set to be zero degree, which means holding the body to be as horizontal as possible, and the rotation speed of wheels is set to be 100 deg/s. Still collect the pitch angle data from the sensing function of 'bushing joint' attached to the body in Simscape, which serves as the 'IMU' in real world. It is worth mentioned here that we only take the data relative to pitch angle, the 'virtual desired posture' signal of roll and stand height are all constant, without PID control. In brief,

this is a single-aim experiment, and the controller only take the data relative to pitch angle into consideration and create a time-varying 'virtual desired pitch angle'.

The pitch angle performances of the wheel-legged vehicle with control and without control are shown in the solid lines of Figure 6-6. Without attitude controller, the vehicle tilts along with the shape of the terrain and the maximum pitch angle can reach nearly 8 degrees, and the peak-to-peak value reaches almost 15 degrees. Obviously, the performance without control is worse in the oscillation amplitude and frequency. The red line illustrates a much smooth curve with smaller amplitude and frequency. The maximum pitch angle with attitude control is only below 0.5 degree.

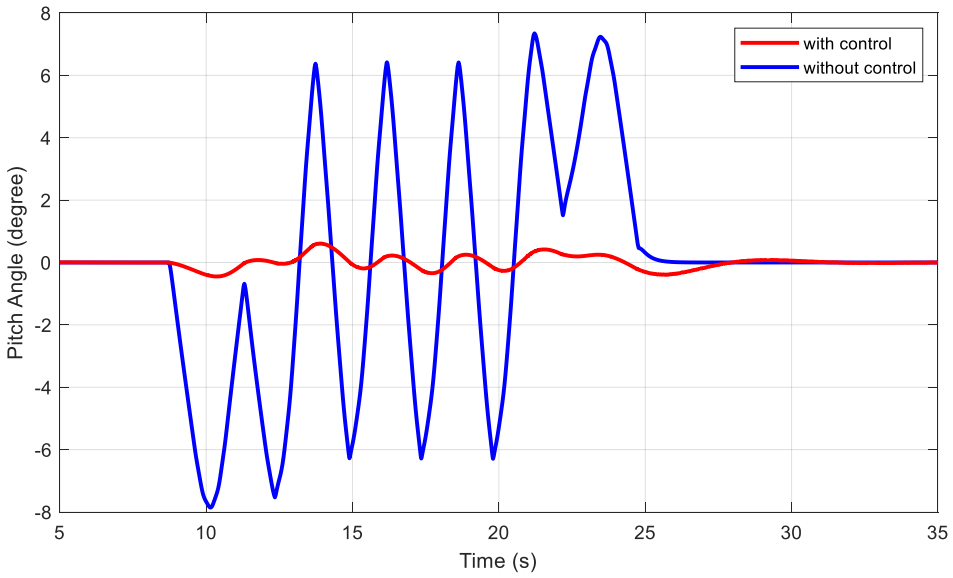

Figure 6-6 Pitch Angle Performance of the Vehicle on Terrain 2

To show the posture more vividly, Figure 6-7 shows how the vehicle behaves on Terrain 2, with control and without control. The body at the bottom keeps horizontal as desired and legs bend according to attitude control algorithm.

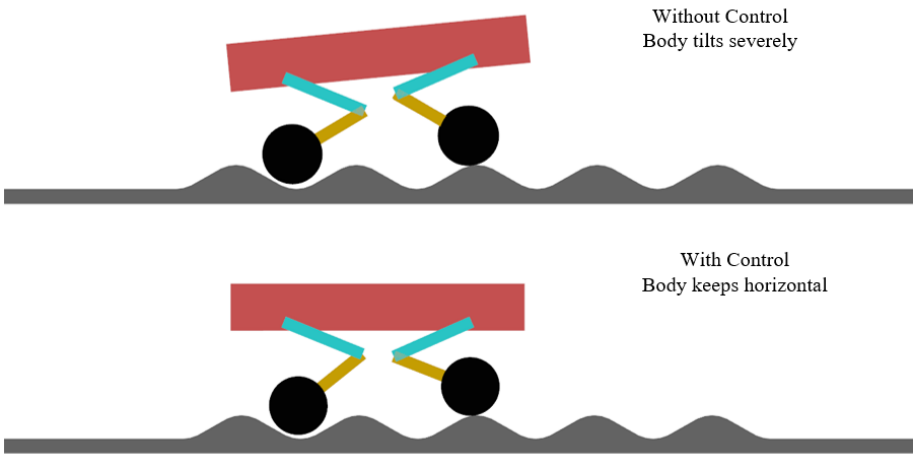

Figure 6-7 Simulation of Vehicle Motion on Terrain 2

6.6 Multi Aims Verification on Terrain 3

Usually, a single attitude parameter cannot ensure the stability of the vehicle. For example, if the pitch angle is controlled in a small range while the roll angle is out of controlled, the vehicle would also show strange attitude that is not stable enough to guarantee the safety of the things it carries. As stated in previous chapters, pitch angle, roll angle and stand height are three common and crucial parameters that directly determine the attitude of the vehicle. Therefore, to keep the wheel-legged vehicle stable in various tough terrains, those three parameters should be controlled at the same time.

Since terrain 2 is symmetric, it is only valid to verify the pitch angle performance. To verify all three posture parameters stated in previous paragraph, a more difficult terrain, terrain 3, is built. As shown in Figure 6-8, the sinewave curve on the left side last 3 periods and leads half period than the ones on the right side. The unsymmetric structure of terrain 3 is more suitable than terrain 2 to verify roll angles.

The aims are maintaining zero roll angle and zero pitch angle of the body when crossing terrain 3 and hold the body stationary along the z axis of the fixed world frame. Similar to the pitch control scheme, 'virtual roll angle' is produced by the sum of desired roll angle and data relative to roll angle collected by IMU, and 'virtual stand height' is produced by the data relative to velocity along z axis. Also define the rotation speed of

wheels are 100 deg/s, the roll, pitch and stand height of the vehicle are shown in Figure 6-9, Figure 6-10, and Figure 6-11 respectively.

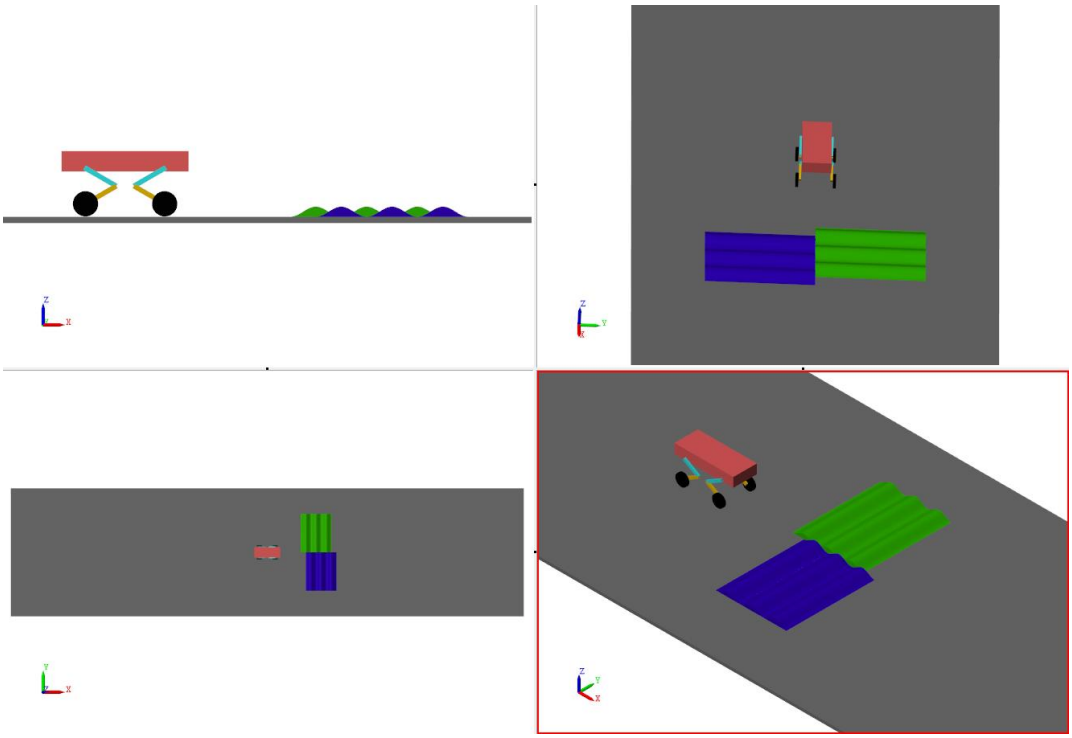

Figure 6-8 Terrain 3: the Unsymmetric Terrain

Figures shows that the attitude control scheme built in this project performs well on terrain 3. The roll angle has been limited in the range from - 0.2 degree to 0.2 degree, which is so tiny that is almost unobservable. However, the roll angle can oscillate from -5 degrees to 5 degrees without attitude control, and the peaks and valleys of the blue lines in Figure 6-9 is much sharper than the red one. Therefore, the roll angel with controller does not swing in a large domain and suffers less shock. The performance of pitch angle is similar to the performance on terrain 2, from - 0.3 degree to 0.3 degree. As for the stand height, Figure 6-11 shows the stand height by measuring the z coordinates of the COM of the body in the fixed world frame. It shows that the absolute height of the vehicle is limited in small domain. The body is raised only 6 millimeters, which is much smaller than the peak-to-peak value of the sinewave.

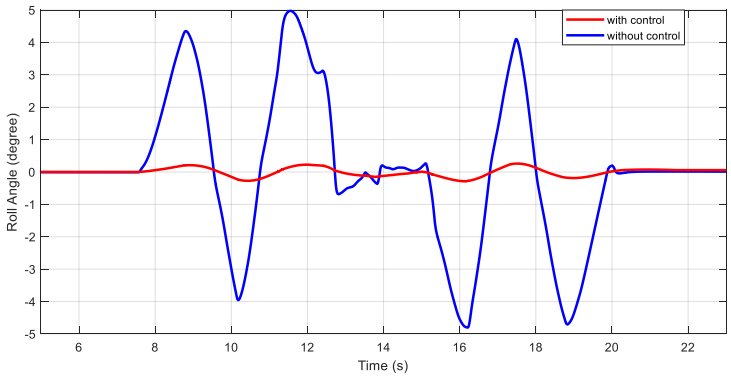

Figure 6-9 Roll Angle Performance of the Vehicle on Terrain 3

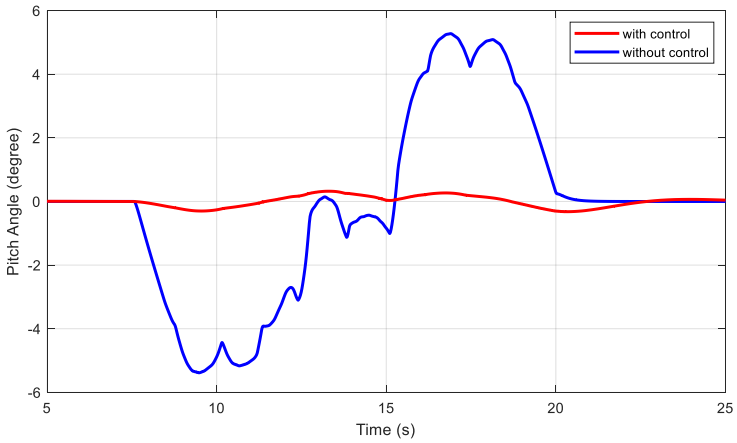

Figure 6-10 Pitch Angle Performance of the Vehicle on Terrain 3

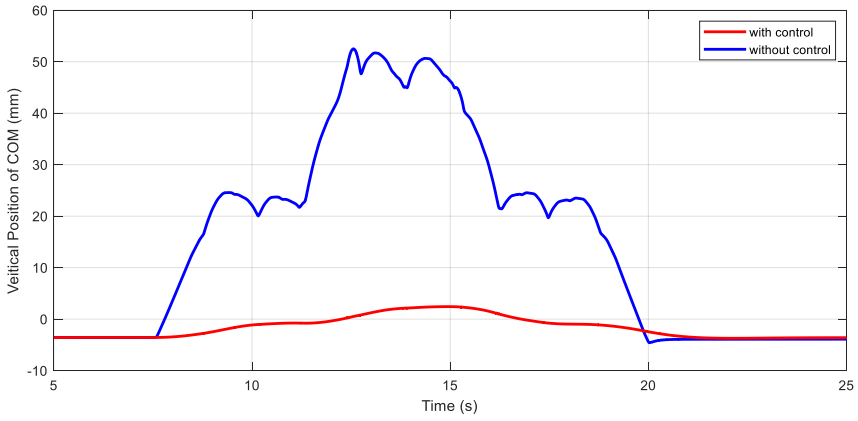

Figure 6-11 Stand Height Performance of the Vehicle on Terrain 3

The attitude of the vehicle on terrain 3 is shown intuitively in Figure 6-12. The left part of the figure shows that the vehicle is suffering large-scale vibrations with large roll angle, and pitch angle. The right part of the figure shows that the vehicle can pass through terrain 3 smoothly with unobservable pitch and roll angle, and the height of the body can even hold on to a fixed altitude that swing between a small domain in z direction.

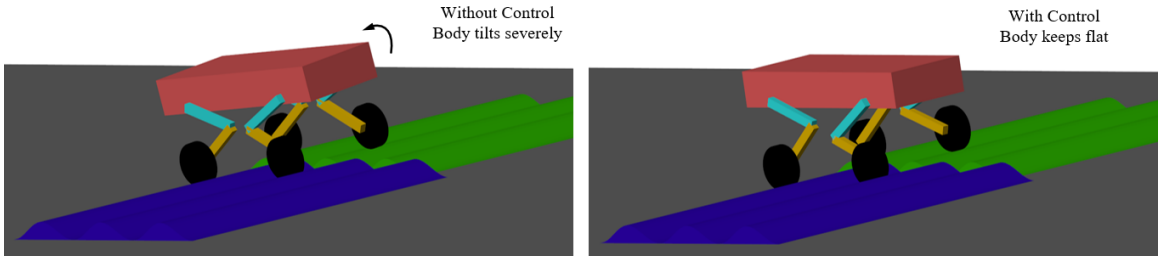

Figure 6-12 Simulation of Vehicle Motion on Terrain 3

Conclusions

The thesis mainly focusses on the forward and inverse kinematics of the leg mechanism of the vehicle, and analyze the dynamic performance of virtual components attached to legs. Furthermore, it introduces an attitude control scheme for the wheel-legged vehicle based on the virtual model control theory, and the Simscape simulation has shown the effectiveness of the control method on sinewave terrains. The detailed analysis process and conclusions are shown below.

Firstly, the background and significance of the analysis on wheel-legged vehicle are emphasized. The advantages and limitations of the motion of wheeled vehicle and legged robots are stated separately. The current research status of the attitude control and modelling theory are also well explained, including the virtual model control theory (VMC) applied in the thesis. Moreover, basic frames have been correctly set, and the 'roll-pitch-yaw' method is defined to analyze the attitude of the vehicle. Applying basic knowledge of homogenous transformation, 'leg vectors' can be calculated according to the desired attitude. It is noticed that, the input desired attitude is always measured from the local ground. With correct local frames on each leg according to D-H convention, the inverse kinematics of the leg mechanism can be derived in geometric way and algebraic way. The leg system of the vehicle can be imagined to a virtual mass-spring-damped system, in two directions. Since the structure parameters of the virtual components are well tuned by the Simscape model, the vehicle performs rationally when accelerating on flat ground or flip from a high altitude.

The attitude control method feeds the data collected from IMU back to the input desired posture. Since the input desired signals to calculate leg vectors are always measured from the local ground, a PID controller has been designed to form appropriate 'virtual desired posture' to make the vehicle performing desired attitude in fixed world frame. The virtual model controller generates torque signals by Jacobian matrix. And a compensate signal formed by inverse kinematics also generates torque signals to decrease steady-state error. The sum of those torques drive the joint motor and the vehicle can adjust the attitude when passing through tough terrains.

Sinewave terrains are built by CAD software to simulate natural tough terrains. The attitude performance of the vehicle on symmetric terrain (terrain 2) and unsymmetric terrain are much better than uncontrolled vehicle, with tiny domains of stand height, pitch angle, and roll angle. Results show that the attitude control scheme is rational and effective. However, there are still many limitations to be improved further, and more intelligent algorithm can be applied to control wheel-legged vehicle.

References

[1] Niu J, Wang H, Shi H, et al. Study on structural modeling and kinematics analysis of a novel wheel-legged rescue robot[J]. International Journal of Advanced Robotic Systems, 2018, 15(1): 1729881417752758.

[2] Du W, Fnadi M, Benamar F. Rolling based locomotion on rough terrain for a wheeled quadruped using centroidal dynamics[J]. Mechanism and Machine Theory, 2020, 153: 103984.

[3] Li J, Wang J, Peng H, et al. Neural fuzzy approximation enhanced autonomous tracking control of the wheel-legged robot under uncertain physical interaction[J]. Neurocomputing, 2020, 410: 342-353.

[4] Jiang H, Xu G, Zeng W, et al. Design and kinematic modeling of a passively-actively transformable mobile robot[J]. Mechanism and Machine Theory, 2019, 142: 103591.

[5] Rollins E, Luntz J, Foessel A, et al. Nomad: a demonstration of the transforming chassis[C]//Proceedings. 1998 IEEE International Conference on Robotics and Automation (Cat. No. 98CH36146). 1998, 1: 611-617IEEE, 1998: 611-617.

[6] Volpe R, Balaram J, Ohm T, et al. Rocky 7: A next generation mars rover prototype[J]. Advanced Robotics, 1996, 11(4): 341-358.

[7] Estier T, Crausaz Y, Merminod B, et al. An innovative space rover with extended climbing abilities[C]//Robotics 2000. 2000: 333-339.

[8] 司马光. 灵活高效的玉兔号月球车[J]. 国际太空, 2013(12): 15-19.

[9] Park H-W, Wensing P M, Kim S. High-speed bounding with the MIT Cheetah 2: Control design and experiments[J]. The International Journal of Robotics Research, 2017, 36(2): 167-192.

[10]Nguyen Q, Powell M J, Katz B, et al. Optimized jumping on the mit cheetah 3 robot[C]//2019 International Conference on Robotics and Automation (ICRA). 2019: 7448-7454IEEE, 2019: 7448-7454.

[11]Katz B, Di Carlo J, Kim S. Mini cheetah: A platform for pushing the limits of dynamic quadruped control[C]//2019 International Conference on Robotics and Automation (ICRA). 2019: 6295-6301IEEE, 2019: 6295-6301.

[12]Katz B G. A low cost modular actuator for dynamic robots[D]. Massachusetts Institute of Technology, 2018.

[13]Raibert M, Blankespoor K, Nelson G, et al. Bigdog, the rough-terrain quadruped robot[J]. IFAC Proceedings Volumes, 2008, 41(2): 10822-10825.

[14]Remy C D, Baur O, Latta M, et al. Walking and crawling with alof-a robot for autonomous locomotion on four legs[M]//Emerging Trends In Mobile Robotics. 2010: 501-508World Scientific, 2010: 501-508.

[15]张秀丽. 四足机器人节律运动及环境适应性的生物控制研究[D]. 北京: 清华大学, 2004.

[16]吴立卫, 刘明宝, 林润华. JTUWM-II 四足步行机器人控制系统的计算机结构[J]. 机器人, 1992, 14(3): 29-32.
[17]张国腾. 四足机器人主动柔顺及对角小跑步态运动控制研究[D]. 山东大学, 2016.
[18]Bogue R. Robots for space exploration[J]. Industrial Robot: An International Journal, 2012.
[19]Hirose S. Variable constraint mechanism and its application for design of mobile robots[J]. The International Journal of Robotics Research, 2000, 19(11): 1126-1138.
[20]BenAmar F, Budanov V, Bidaud P, et al. A high mobility redundantly actuated mini-rover for self adaptation to terrain characteristics[C]//3rd Int. Conference on Climbing and Walking Robots (CLAWAR'00). 2000: 105-112.
[21]Takita Y, Shimoi N, Date H. Development of a wheeled mobile robot" octal wheel" realized climbing up and down stairs[C]//2004 IEEE/RSJ International Conference on Intelligent Robots and Systems (IROS)(IEEE Cat. No. 04CH37566). 2004, 3: 2440-2445IEEE, 2004: 2440-2445.
[22]Xu K, Wang S, Yue B, et al. Adaptive impedance control with variable target stiffness for wheel-legged robot on complex unknown terrain[J]. Mechatronics, 2020, 69: 102388.
[23]Grand C, Benamar F, Plumet F, et al. Stability and traction optimization of a reconfigurable wheel-legged robot[J]. The International Journal of Robotics Research, 2004, 23(10-11): 1041-1058.
[24]Klemm V, Morra A, Salzmann C, et al. Ascento: A Two-Wheeled Jumping Robot[C]//2019 International Conference on Robotics and Automation (ICRA). 2019: 7515-7521Montreal, QC, Canada: IEEE, 2019: 7515-7521.
[25]Klemm V, Morra A, Gulich L, et al. LQR-assisted whole-body control of a wheeled bipedal robot with kinematic loops[J]. IEEE Robotics and Automation Letters, 2020, 5(2): 3745-3752.
[26]谢惠祥. 四足机器人对角小跑步态虚拟模型直觉控制方法研究[D]. 国防科学技术大学, 2015.
[27]Pratt J, Chew C-M, Torres A, et al. Virtual Model Control: An Intuitive Approach for Bipedal Locomotion[J]. The International Journal of Robotics Research, 2001, 20(2): 129-143.
[28]Chew C-M, Pratt G A. Dynamic bipedal walking assisted by learning[J]. Robotica, 2002, 20(5): 477-491.
[29]Spong M W, Hutchinson S, Vidyasagar M, et al. Robot modeling and control[M]. Wiley New York, 2006.
[30]Liu H, Liu B, Han Z, et al. Attitude control strategy for unmanned wheel-legged hybrid vehicles considering the contact of the wheels and ground[J]. Proceedings of the Institution of Mechanical Engineers, Part D: Journal of Automobile Engineering, 2021: 09544070211058382.
[31]Ni L, Ma F, Wu L. Posture control of a four-wheel-legged robot with a suspension

system[J]. IEEE Access, 2020, 8: 152790-152804.
[32]陈佳品, 程君实, 席裕庚. 基于虚拟模型的四足机器人直觉控制[J]. 上海交通大学学报, 2002, 36(8): 1150-1154.

Acknowledgement

In the past four years, I have gained plenty of precious knowledge that I am curious about since my childhood. The four-years life in college makes me more mature, and it's lucky for us to enjoy one of the most beautiful and habitable campus in Liangxiang. I will never forget my passions in watching Formula 1 racing cars and the feeling of pressing the throttle of the Baja racing car. Glad to get the drive license in 2019, I can drive cars to travel and enjoy the landscape beside roads. I hope the scenery in the following of my life will be much more spectacular.

I am grateful to my dear parents, who raise me up and always stand behind me. Although they are not skilled in academic knowledge, the experience and character they impart to me are far more helpful. Thanks to Professor Hui Liu and Lijin Han, who guide me to do the research described in this thesis. They help me a lot in research technique and their spirit in academic field impressed me a lot. Thanks to Teacher Mindi Zhang who cares about the daily life and academic performance of the students in our class. Besides, I am grateful to every dear friend who accompanies me for such a long time and share your happiness and sadness with me. I will keep progressing and bring more happiness to everyone I concern.